Tuesday Posters

Poster-Tu01

Optical spectroscopy in high magnetic fields

S. Georges,[1] Z. Yang,[1] A. Surrente,[1] N. Bruyant,[1] and P. Plochocka[1]

[1] *Laboratoire National des Champs Magnétiques Intenses, CNRS-UGA-UPS-INSA, Toulouse, France*

Optical UV-Visible spectroscopy in high magnetic field is a powerful tool to study various semiconductor samples, for example to investigate the exciton binding energies in hybrids perovskites[1] or to study the photoluminescence of colors center in synthetic diamonds [2]. We present the measurement systems available to external users in Laboratoire National des Champs Magnétiques Intenses, Toulouse, France.

The classical arrangement of instrument is described in fig. 1, it consists of a light source injected into a first optical fiber, the light coming back from the sample is then analyzed by a spectrometer and recorded by a fast camera. We offer our users, broadband light sources in the UV to NIR range and spectrometer equipped with CCD and InGaAS cameras.
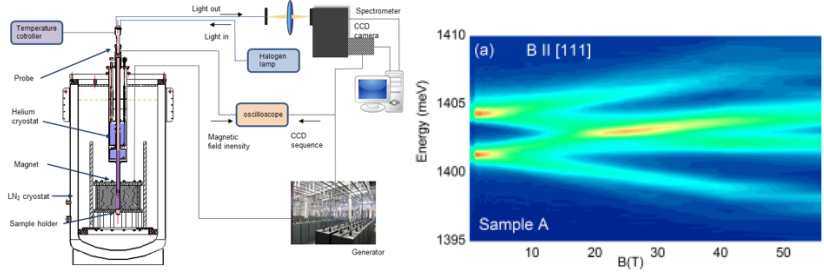

FIG. 1. *Right: Representative T = 4.2 K magneto- photoluminescence spectra in the Faraday configuration of the 1.4 eV Ni color center in HPHT synthetic diamond from [2]. Macro-PL with B ⊥ [111] collected from the (111) face. Left: Typical spectroscopy setup for a UV-Vis spectroscopy experiment in pulsed magnetic field : Light source, optical probe, fast spectrometer and DAQ.*

The key point of a successful measurement in pulsed field is the sample to optical fiber coupling. We designed a wide range of probes for 70T, 80T and 90T magnets in Faraday or Voigt configuration, for transmission, reflectivity and photoluminescence. Coupling from fiber to sample can be accomplished using fiber bundles with well chosen NA, graded index lenses or spherical lenses (see fig. 2).
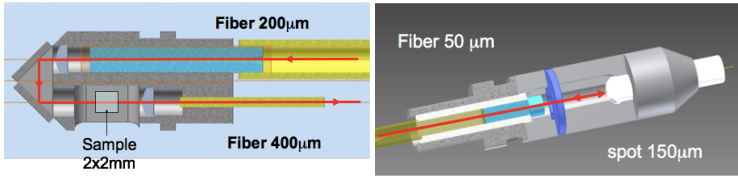

FIG. 2. *CAD Drawing of the typical samples holders: on the left 80T transmission probe allowing 3x3 mm samples to be measured in transmission with optional incident and transmitted polarizers in the UV-VIS range , right: 80T probe allowing to measure photoluminescence on 1.5x1.5 mm samples*

To build pulsed field optical probes we use only non-magnetic and non-conductive materials. To mesure magnetic field, a calibrated pick-up coil is used and a diode temperature sensor is placed in the vicinity of the sample. The optical probes are placed in helium bath cryostats with temperatures ranges from 1.4K to 300K at the center of the pulsed magnet. The data acquisition of spectra is synchronized with magnetic fields measurement allowing the reconstruction of magneto-optics spectra.

[1] Yang, Z. *et al.*, J. Phys. Chem. Lett., American Chemical Society, 2017, **8** , 1851-1855

[2] Plochocka, P. *et al.*, Phys. Rev. B, American Physical Society, 2012 , **86**, 045203

Poster-Tu02

Valley polarization of monolayer MoSe₂ and WSe₂ in high magnetic fields

Mariana V. Ballottin,[1] Anatolie A. Mitioglu,[1] Andrés Granados del Águila,[1,2] Philipp Nagler,[3] Gerd Plechinger,[3] Christian Schüller,[3] Tobias Korn,[3] and Peter C. M. Christianen[1]

[1] *High Field Magnet Laboratory (HFML - EMFL),*
Radboud University, Nijmegen, The Netherlands

[2] *Division of Physics and Applied Physics, School of Physical and*
Mathematical Sciences, Nanyang Technological University, Singapore

[3] *Institut für Experimentelle und Angewandte Physik, Universität Regensburg, Regensburg, Germany*

Semiconducting monolayer (ML) transition-metal dichalcogenides (TMDs) exhibit interesting optical properties related to spin and valley physics. These materials have a direct band gap at degenerate, but inequivalent, valleys at the K^+ and K^- points of the Brillouin zone. Broken inversion symmetry and a strong spin-orbit interaction couple the spin and valley degrees of freedom, which permits addressing the distinct valleys by circularly polarized (σ^+ or σ^-) light. Excitation with $\sigma^+(\sigma^-)$ light leads to a predominantly $\sigma^+(\sigma^-)$-polarized emission of excitons, even at zero magnetic field [1]. The precise amount of this so-called valley polarization (*VP*) is directly related to the competition of intra- and inter-valley scattering processes and depends on the type of TMD material, the laser excitation energy and the strength of an applied magnetic field [2].

We have measured the valley polarization of ML MoSe₂ and WSe₂ in magnetic fields up to 30 T. In our experiments we have used four different combinations of the circular polarization of the excitation and detection channels, which allows us to distinguish between intra- and inter-valley relaxation. Two excitation energies are used; one far above the exciton emission (non-resonant excitation) and one close to it (near-resonant excitation). MoSe₂ does not show any *VP* at 0 T and non-resonant excitation, indicative of efficient inter-valley scattering. Its *VP* increases with field, irrespective of the excitation polarization, reaching 50% at 30 T, corresponding to a *VP* that is purely driven by the occupation of the Zeeman split exciton levels (Figure 1, green circles). In contrast, under near-resonant excitation MoSe₂ displays a *VP* of 20% at 0 T, which increases with field strength (Figure 1, red circles), saturating to a *VP* value close to that of the curve measured with non-resonant excitation. In this case, the *VP* is partially driven by the excitation polarization and presents a competition between occupation and excitation effects. Remarkably, at 0 T and non-resonant excitation WSe₂ shows a *VP* of 30% (Figure 1, green squares), which remains roughly constant with increasing magnetic field, demonstrating that the field has little influence on the inter-valley scattering of the photo-excited excitons. We explain our *VP* data with a rate equation model using the inter- and intra-valley scattering times (τ_{intra} and τ_{intra}) as fitting parameters, relative to the exciton radiative lifetime. We attribute the differences in the *VP* properties of the Mo- and W-based TMDs to the reversed order of their spin levels in the conduction band. This leads to a bright exciton ground state in ML MoSe₂ and a dark exciton ground state in WSe₂ [3] and modifies the scattering rates due to phonons and the electron-hole exchange interaction.
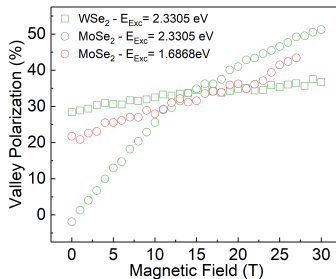

FIG. 1. *Exciton valley polarization of ML MoSe₂ and WSe₂ as a function of magnetic field at 4.5 K. The excitation is circularly polarized. Non-resonant excitation (2.3305 eV) for WSe₂ (green squares) and MoSe₂ (green circles). Near-resonant excitation (1.6868 eV) for MoSe₂ (red circles).*

[1] K. F. Mak *et al.*, Nat. Nanotech. **7**, 494 (2012).
[2] G. Wang *et al.*, 2D Materials, **2**, 034002 (2015).
[3] M. Baranowski *et al.*, 2D Materials, **4**, 2, (2017).

Poster-Tu03

Diamagnetic shift of exciton and trion transitions in MoS_2 and $MoSe_2$ monolayers

S. Zelewski,[1,2] A. Surrente,[2] M. Baranowski,[1,2] A. A. Mitioglu,[3] M. V. Ballottin,[3] P. C. M. Christianen,[3] D. Dumcenco,[4] Y.C. Kung,[4] D. K. Maude,[2] A. Kis,[4] and P. Plochocka[2]

[1]*Department of Experimental Physics, Faculty of Fundamental Problems of Technology, Wroclaw University of Science and Technology, Wroclaw, Poland*

[2]*Laboratoire National des Champs Magnétiques Intenses, UPR 3228, CNRS-UGA-UPS-INSA, Grenoble and Toulouse, France*

[3]*High Field Magnet Laboratory (HFML – EMFL), Radboud University, 6525 ED Nijmegen, The Netherlands*

[4]*Electrical Engineering Institute and Institute of Materials Science and Engineering, École Polytechnique Fédérale de Lausanne, CH-1015 Lausanne, Switzerland*

Monolayer transition metal dichalcogenides (TMDs) have recently emerged as an exciting material system with unique electrical and optical properties that are absent in their bulk and few-layer forms. The lack of inversion symmetry together with strong spin-orbit coupling results in intriguing coupled spin-valley physics which can be explored using optical spectroscopy. The optical properties of single layer TMDs are dominated by excitonic effects. The reduced dielectric screening together with two-dimensional character of monolayer TMDs results in a huge exciton binding energy (in the range of a few hundred meV). Therefore, quantifying the properties of excitons is important to understand the physics of TMDs.

Magneto-optical spectroscopy provides an efficient tool for studying exciton properties. The shift of the exciton transition energy in magnetic field is directly related to the extent of the wave-function, reduced mass, and magnetic moment, which are essential information for benchmarking theoretical models. While the determination of the exciton Zeeman splitting is relatively easy, a reliable determination of the diamagnetic shift is more challenging due to the large exciton binding energy in these 2D materials. To date, the diamagnetic shift of the exciton transition was observed only in WS_2 and WSe_2 [1] due to their superior optical quality.

Here we report on the observation of the diamagnetic shift of the ground state excitonic transition in MoS_2 and $MoSe_2$ monolayers studied in pulsed magnetic fields up to 70 T and static field up to 30T. In addition, we have determined the diamagnetic shift of the charged exciton in $MoSe_2$. To the best of our knowledge this is the first observation of a quadratic (diamagnetic) shift of excitonic transitions in molybdenum-based materials. The non-local dielectric screening model was used to analyse the experimental results to in order to estimate the extent of the exciton wave function together with its reduced mass.
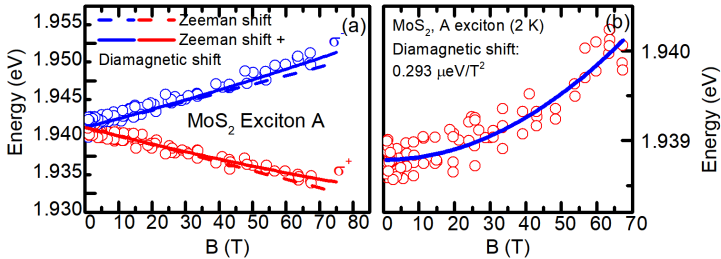

FIG. 1. *(a) MoS_2 A exciton transition energy as function of magnetic field for σ^+ and σ^- polarized light reveals a large Zeeman splitting. (b) Average value of A exciton energy as a function of magnetic field showing a small diamagnetic shift.*

[1] Stier *et al.*, Nat. Commun. **7**, 10643, (2016) and Phys. Rev. Lett. **120**, 057405, (2018)

Poster-Tu04

Ultrahigh magnetic field spectroscopy reveals the band structure of the 3D topological insulator Bi_2Se_3

A. Miyata,[1] Z. Yang,[1] A. Surrente,[1] O. Drachenko,[1] D. K. Maude,[1] O. Portugall,[1] L. B. Duffy,[2] T. Hesjedal,[2] P. Plochocka,[1] and R. J. Nicholas[2]

[1]*Laboratoire National des Champs Magnetiques Intenses, CNRS-UGA-UPS-INSA, Toulouse, France*

[2]*Clarendon Laboratory, University of Oxford, Oxford, UK*

The 3D topological insulator Bi_2Se_3 has been intensively investigated to understand the unconventional properties arising from the topological surface states. However, there have been few experimental studies of their band structures in the bulk, despite the fact that the origin of topological surface states is critically dependent on the band inversion in the bulk crystal. Recently magneto-optical studies revealed the band character in the bulk of Bi_2Se_3, which has been described by the massive Dirac Hamiltonian with a negative mass term. Remarkably, the observed evolution of the Landau-level energies in Bi_2Se_3 remain linear even up to 32 T, indicating that for the energies investigated ($E < 0.6$ eV), the band dispersion in the bulk of Bi_2Se_3 is almost perfectly parabolic [1].

We have conducted magneto-optical studies of single crystal thin-film Bi_2Se_3 using ultrahigh magnetic fields up to 150 T over a wide range of energies (0.55 to 2.2 eV) to investigate its bulk band structure.

Figure 1(a) shows the Landau level fan chart combining our transmission data with the low-energy data in Ref. 1. The interband Landau level transitions calculated using the 4×4 massive Dirac Hamiltonian reproduce the data perfectly, with a band gap of 2Δ=0.19 eV, Fermi velocity $v_D = 0.465 \pm 0.05 \times 10^6$ ms^{-1}, negative mass term $M = -17 \pm 0.5$ eVÅ^2, electron-hole asymmetry parameter $C = 3 \pm 0.5$ eVÅ^2. In Fig. 1(b), the interband Landau level transitions, with different indexes, are scaled into the same energy-momentum dispersion of Bi_2Se_3. For energies above 0.6 eV a clear deviation from the simple parabolic model is observed reflecting the transition towards a $\sqrt{B}$ dependence of Dirac fermions.

At higher energies around 0.99 and 1.6 eV, additional strong absorptions are observed as the lowest interband Landau level transitions of the 2nd and 3rd bandgaps with clearly resolved spin-orbit splittings. From their temperature and magnetic field dependence, they are assigned as excitonic band edge transitions for these higher band gaps [2].
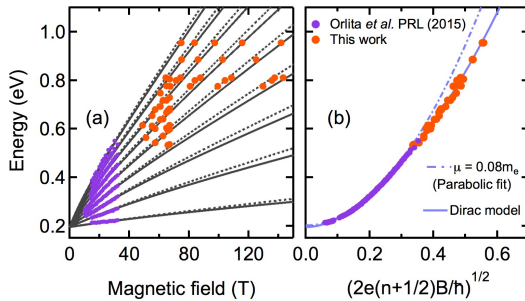

FIG. 1. *(a) Low-temperature interband Landau-level fan chart for the first (fundamental) band gap in Bi_2Se_3. Dashed and solid lines are interband Landau levels obtained by the 4×4 massive Dirac Hamiltonian with electron-hole asymmetry. (b) Energy-momentum dispersion of Bi_2Se_3. The dashed line shows the fitting for parabolic dispersion.*

[1] Orlita *et al.* Phys. Rev. Lett. **114**, 186401 (2015).

[2] Miyata *et al.* Phys. Rev. B **96**, 121111(R) (2017).

Poster-Tu05

Controlling ferroelectric distortion with magnetic field in the multiferroic GeMnTe semiconductor

H. Przybylińska,[1] V. Volobuev,[2,3] G. Springholz,[2] A. Grochot,[2] W. Jantsch,[2] G. Bauer,[2] and A. Ney[2]

[1]*Institute of Physics, Polish Academy of Sciences, Warsaw, Poland*

[2]*Institute of Semiconductor and Solid State Physics, Johannes Kepler University, Linz, Austria*

[3]*International Research Centre MagTop, Warsaw, Poland*

GeMnTe is one of the rare materials that, at low temperatures, are simultaneously ferroelectric (FE) and ferromagnetic (FM) and thus fulfills a necessary condition for the appearance of multiferroicity. Ferromagnetism is induced by interaction of free holes with the magnetic moments of Mn ions, while the FE moment results from relative displacement of the cation and anion fcc sublattices along a <111> body diagonal, accompanied by transition from the cubic to the rhombohedral structure. In bulk crystals all <111> directions are equally probable, whereas in thin layers grown on (111) BaF_2 substrates biaxial strain leads to preferential orientation of the FE distortion perpendicular to the layer surface [1]. In order to enable ferroelectric distortions along other body diagonal directions InP, which is almost lattice matched to GeMnTe, was chosen as a substrate.

The present results were obtained on a series of 500 nm thick $Ge_{1-x}Mn_xTe$ layers grown by molecular beam epitaxy (MBE) on BaF_2 (111) and InP (111)A surface substrates. The Mn content, x, was varied between 0.2 and 0.4. The growth on both substrates was conducted simultaneously in the MBE chamber to ensure by the same growth conditions, similar Mn content and free carrier concentrations. The room temperature lattice constants as well as corresponding FE distortion directions were determined by high resolution x-ray diffraction reciprocal space mapping. The magnetic properties of the layers were derived from SQUID magnetometry. The changes in magnetocrystalline anisotropy were monitored by angular dependent ferromagnetic resonance (FMR) measurements performed at 9.5 GHz with use of a Bruker ESR spectrometer.

X-ray diffraction mapping at room temperature confirmed that in the GeMnTe/InP system FE distortions along the oblique <111> directions occur considerably more frequently than in the corresponding GeMnTe/BaF_2 layers. In the low temperature ferromagnetic phase, however, only FE distortion along one of the three oblique body diagonals was observed, in contrast to samples grown on BaF_2 where the distortion axis is always perpendicular to the layer surface. Moreover, the specific oblique <111> distortion axis was uniquely determined by the orientation of the applied magnetic field. We demonstrate multiferroic behavior in the GeMnTe/InP layers by the observed complete switching of the spontaneous electric dipole moment from one of the oblique <111> axis to another one induced by the appropriate change of the direction of the applied magnetic field.

[1] H. Przybylińska *et al*., Phys. Rev. Lett. **112**, 047202, (2014)

Poster-Tu06

Bright exciton fine structure splitting in bulk MAPbBr$_3$ crystal

M. Baranowski,[1, 2] K. Galkowski,[1, 3] A. Surrente,[1] J. Urban,[1] L. Kłopotowski,[4] S. Maćkowski,[3]
D. K. Maude,[1] P. K. Nayak,[5] M. Dollmann,[5] H. J. Snaith,[5] R. J. Nicholas,[5] and P. Plochocka[1]

[1]*Laboratoire National des Champs Magnétiques Intenses,*
UPR 3228, CNRS-UGA-UPS-INSA, Grenoble and Toulouse, France

[2]*Department of Experimental Physics, Faculty of Fundamental Problems of Technology,*
Wroclaw University of Science and Technology, Wroclaw, Poland

[3]*Institute of Physics, Faculty of Physics, Astronomy and Informatics,*
Nicolaus Copernicus University, 5th Grudziadzka St., 87-100 Torun, Poland

[4]*Institute of Physics, Polish Academy of Sciences, al. Lotnikow 32/46, 02-668 Warsaw, Poland*

[5]*University of Oxford, Clarendon Laboratory, Parks Road, Oxford, OX1 3PU, United Kingdom*

The exchange interaction between the electron and the hole lifts the degeneracy between the dark singlet and bright triplet excitonic states. The bright states can be further split in the presence of a symmetry breaking leading to bright excitonic fine structure. To date, investigations have largely focused on semiconductor nanostructures where quantum confinement greatly enhances the exchange interaction and breaks the symmetry of the system.

To the best of our knowledge, the fine structure splitting of the bright exciton triplet state has never been observed in a bulk semiconductor. Here we report on the observation a giant FSS of the bright 1s exciton states in a bulk high quality MAPbBr$_3$ single crystal. We have performed a detailed magneto-optical investigation to reveal the FSS as large as 200μeV. Such a large FSS in bulk material indicates a strong symmetry breaking in the orthorhombic crystal lattice and/or significant Rashba enhancement of the FSS. For our bulk single crystal quantum confinement can be excluded so our results give direct insight into the FSS related solely to crystal structure of bulk MAPbBr$_3$.
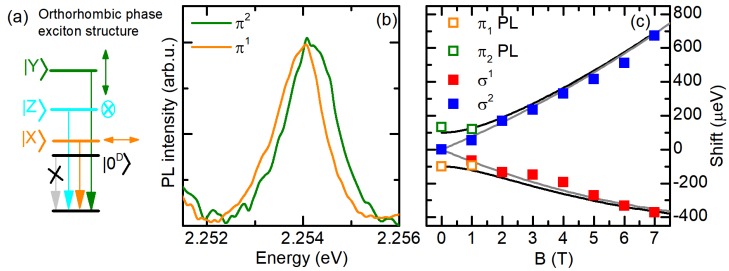

FIG. 1. *(a) Schematic showing exciton fine structure in the orthorhombic phase. (b) two linearly polarized components of photoluminescence emission. (c) dependence of PL peak position as a function on magnetic field detected with linear and circular polarization base.*

Our investigation provide valuable insight for the future understanding of the contribution of different mechanisms, such as confinement anisotropy or Rashba effect, to the FSS of excitons in perovskite based nanostructures [2]. This represent a crucial step in the understanding of fine structure splitting in lead-halide perovskites.

[1] M. Bayer *et al.*, Phys. Rev. B **65**, 195315, (2002)

[2] M. A. Becker *et al.*, Nature **553**, 189. (2018)

Poster-Tu07

Investigation of transport properties on PbTe/Pb$_{1-x}$Sn$_x$Te heterostructures

S. Nakamatsu[1], M. L. Peres[1], D. A. W. Soares[1], C. I. Fornari[2], P. H. O. Rappl[2], E. Abramof[2]

[1]*Instituto de Física e Química, Universidade Federal de Itajubá, Itajubá, MG CEP 37500-903, Brazil*

[2]*Laboratório Associado de Sensores e Materiais, Instituto Nacional de Pesquisas Espaciais, São José dos Campos, PB 515, SP CEP 12201-970, Brazil*

PbTe compounds have been used for the development of infrared photodetectors and diode lasers [1] over the decades. Introduction of Sn atoms makes this material even more interesting for practical applications as well as from the basics physics point of view. According to the band inversion model, the gap of Pb$_{1-x}$Sn$_x$Te decreases as Sn composition increases, and vanishes for an intermediate alloy composition. Further increasing of Sn concentration leads to the band inversion and the energy gap starts to increase up to the SnTe value. Very recently, it was discovered that in the region of band inversion, transition from metallic to crystalline topological insulator (TCI) occurs [3]. Recent theoretical work demonstrated that the PbTe/Pb$_{1-x}$Sn$_x$Te heterostructures can present topological states in the interface of the heterojunction. Such an interface of PbTe and Pb$_{1-x}$Sn$_x$Te, at which four Dirac cones appear, is analogous to the surface of a weak TI [4]. In this work we perform electrical characterization in PbTe/Pb$_{1-x}$Sn$_x$Te films for different values of *x* close to the band inversion in order to verify the existence a single gapless helical state in the [111] direction at the heterostructure interface. Morfological characterization will also be performed in order to provide a detailed view of these new structures. We hope that this work contribute to a better comprehension of the nature of topological insulators based on IV-VI compounds.

References

[1] I. U. Arachchige and M. G. Kanatzidis, **Nano Lett**. 9 (4), 1583 (2009)

[2] R. Jaramillo et al, **Jour. Appl. Phys**. **119**, 035101 (2016)

[3] P. Dziawa, **Nature Materials** 11, 1023 (2012)

Poster-Tu08

Magnetotransport measurements in Bi$_2$Te$_3$/BaF$_2$ nanostructures

Marcelos Peres,[1] Sandra Nakamatsu,[1] Demétrio Soares,[1] Celso Fornari,[2] Eduardo Abramof[2] and Paulo Rappl[2]

[1]*Federal University of Itajubá, UNIFEI, Minas Gerais, Brazil*

[2] *Associated Laboratory of Sensors and Materials, INPE, São José dos Campos, Brazil*

In this work we present magnetotransport measurements performed in a series of films of Bi$_2$Te$_3$ with thickness varying from 8nm to 200nm with BaF$_2$ cap layers. We expect that adding the cap layer we can reduce oxidation process preserving the integrity of films surface since Dirac states are highly surface-sensitivity [1].

Hall effect will be performed on the samples in the range of 300 – 1.8K to provide a full description of transport parameters. Magnetorresistance measurements (MR) will be performed in the same temperature range to investigate the presence of spin-orbit coupling effects. The analysis of MR using the available theoretical models can indicate the existence of transport via bulk or surface states. More specifically, using a two-dimensional (2D) modified Dirac model it is possible to describe the contribution to MR in both the surface bands and the lowest 2D bulk subbands of a topological insulator thin film [2]. Preliminary results are presented in figure 1. In Fig. 1(a), MR measurements show the presence of spin-orbit coupling, where there is an abrupt increase of MR close to 0T. The inset shows the measurement up to 9T, where MR present a linear behaviour. Fig. 1(b) shows the electrical resistance (R) as a function of temperature indicating a drop in R for T below 4K, which corroborates the effect observed in Fig. 1(a).
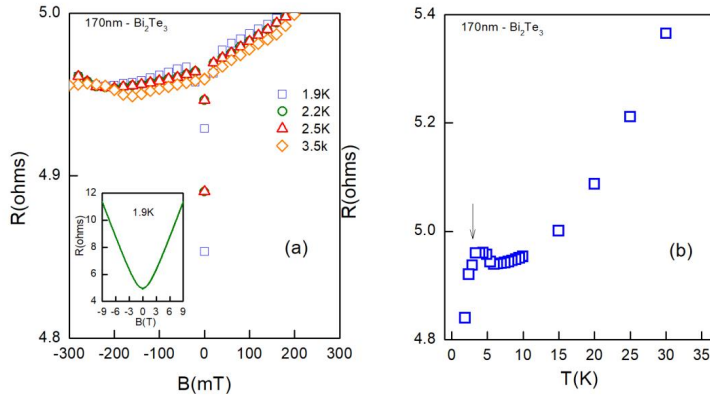

FIG. 1. (a) Magnetorresistance of Bi$_2$Te$_3$ film with thickness of 170nm for 1.9K, 2.2K, 2.5K and 3.5K. There is an abrupt increase of MR close to B=0T indicating the presence of strong spin-orbit coupling. (b) Electrical resistance as a function of temperature. For temperatures smaller than 4K, there is a clear drop in resistance (see arrow) also indicating the presence of strong spin orbit-coupling.

[1] Conor R. Thomas et al. *Chem. Mater.* **28**, (1), 35, (2016)
[2] Hai-Zhou Lu and Shun-Qing Shen, Physical Review B **84**, 125138 (2011)

Poster-Tu09

Effective g-factor in tunnel-coupled III-V semiconductor quantum wells

M. A. T. Sandoval,[1] J. H. L. Padilla,[1] A. Ferreira da Silva,[1] E. A. de Andrada e Silva,[2] and G. C. La Rocca[3]

[1] *Instituto de Física, Universidade Federal da Bahia, 40210-340, Salvador, Bahia, Brazil*

[2] *Instituto Nacional de Pesquisas Espaciais, 12201-970, São José dos Campos, São Paulo, Brazil*

[3] *Scuola Normale Superiore and CNISM, Piazza dei Cavalieri 7, I-56126, Pisa, Italy*

With the development of spintronics and the increasing interest in new schemes for quantum computation, including the use of Majorana fermions, the physics of the effective electron g-factor and its renormalization by the confining potential in semiconductor nanostructures is becoming of crucial importance for the design of new devices. However, even for simple GaAs quantum wells (QWs), we are still facing difficulties; in particular, there is no good agreement between theory [1,2] and experiment [3] for the g-factor anisotropy which is introduced by the confining potential and is the main mesoscopic effect in the effective g-factor tensor. In this work, we consider a more general system with tunnel-coupled quantum wells, and present a simple perturbation but complete envelope-function solution for the electron effective g-factor, based on Kane's 8×8 model for the bulk. Both, symmetric and asymmetric structures are considered, with parameters L_w and L_b (i.e. the width of the wells and the width of the inter-well barrier) varying from zero to infinity, covering different single-QW limits. In the Figure below we show the obtained anisotropy (difference between the longitudinal and transverse g-factors) for symmetric and asymmetric *InGaAs* double QW structures (DQW), (a) and (b) respectively; the asymmetry coming from the use of an infinite barrier in one side only. Among the interesting features observed, we note the known single QW behaviour for large L_b (when the coupling goes to zero), where the g-factor anisotropy as a function of L_w is seen to start from zero, to reach a maximum and then to return slowly to zero, as L_w is increased (from zero). This single QW behaviour is exactly reproduced also when L_b goes to zero. Comparing both maps, one sees that an important effect of the structure inversion asymmetry is the appearance of negative anisotropies at small values of L_b and L_w, which can be easily understood with the present solution [2]. Such DQW structures form exellent testing ground for the theory and we argue that the overall consistency of the results in the whole range of parameters indicates consistency also of the present solution for the effective g-factor. These anisotropy maps serve as a guide for the observation and manipulation of the electron g-factor in semiconductor DQWs, and in general nanostructures as well.
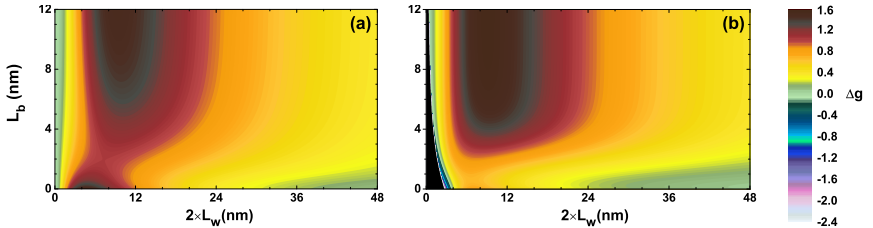

FIG. 1. *Map of the calculated g-factor anisotropy in InGaAs/InP DQW structures, in the structure parameter space, i.e. as a function of L_b (inter-well barrier width) and L_w (width of the wells). In (a) we show the results for symmetric InP/InGaAs/InP/InGaAs/InP DQWs, and in (b) those for asymmetric Insulator/InGaAs/InP/InGaAs/InP DQWs. The g-factor anisotropy is given by the color code on the right, including both positive and negative values.*

[1] A. A. Kiselev and E. L. Ivchenko, Sov. Phys. Semicond., **26**, 827, (1992).

[2] M. A. T. Sandoval *et al.*, Semicond. Sci. Technol., **31**, 115008, (2016).

[3] P. Le Jeune *et al.*, Semicond. Sci. Technol., **12**, 380, (1997); A. Malinowski and R. T. Harley, Phys. Rev. B, **62**, 2051, (2000).

Poster-Tu10

Quantum interference of surface states in Bi-Sb nanowires

L.A Konopko,[1] A.A. Nikolaeva,[1] T.E. Huber,[2] and K. Rogacki[3]

[1] *Ghitu Institute of Electronic Engineering and Nanotechnology, Chisinau, MD-2028, Republic of Moldova*

[2] *Department of Chemistry, Howard University, DC 20059, Washington, U.S.A*

[3] *Institute of Low Temperatures and Structural Research, PAS, Wroclaw 50950, Poland*

Bismuth is a semimetal with strong spin-orbit interactions. Substituting bismuth with antimony changes the critical energies of the band structure. At concentrations greater than $x = 0.09$, the system develops into a direct-gap insulator, the low-energy physics of which is dominated by the spin-orbit coupled Dirac particles at L. Here we study Topological Insulator (TI) $Bi_{1-x}Sb_x$ nanowires with $x = 0.17$, that in the bulk, are semiconductors with an L-point gap of 21 meV. Individual $Bi_{0.83}Sb_{0.17}$ nanowires were fabricated using the Ulitovsky technique. Nanowire samples with diameters ranging from 75 nm to 1.1 μm were prepared. The nanowires are single crystals with $(10\bar{1}1)$ orientation along the wire axis. With the Ulitovsky technique owing to the high frequency stirring and high speed crystallization ($> 10^3$ K/s) involved it is possible to obtain homogeneous monocrystalline $Bi_{0.83}Sb_{0.17}$ nanowires. The transport properties of TI $Bi_{0.83}Sb_{0.17}$ nanowires were investigated earlier [1]. The resistance of the samples was increased with decreasing temperature, but a decrease in resistance was observed at low temperatures. This effect is a clear manifestation of TI properties (i.e., the presence of a highly conducting zone on the TI surface). From the linear dependence of the nanowire conductance on nanowire diameter at $T = 4.2$ K, the square resistance R_{sq} of the surface states of the nanowires was obtained ($R_{sq} = 70$ Ohm). We investigate the magnetoresistance (MR) of $Bi_{0.83}Sb_{0.17}$ nanowires at various magnetic field orientations. Shubnikov-de Haas (SdH) oscillations are observed in $Bi_{0.83}Sb_{0.17}$ nanowires with diameter $d = 200$ nm at $T = 1.5$ K and 3 K, demonstrating the existence of high mobility ($\mu_S = 26700$ - 47000 cm^{2}V^{-1}s^{-1}) two-dimensional (2D) carriers in the surface areas of the nanowires, which are nearly perpendicular to the C_3 axis. In thin $Bi_{0.83}Sb_{0.17}$ nanowires ($d \leq 100$ nm) at low temperatures (1.5 K $\leq T < 5$ K), we discovered the Aharonov Bohm (AB) [2] oscillations of longitudinal MR with two periods - one flux quantum, Φ_0 and half of flux quantum, $\Phi_0/2$, ($\Delta B_1 = \Phi_0/S$, $\Delta B_2 = \Phi_0/2S$, where S is the cross-sectional area of the nanowire). The periods ΔB depend on the inclination angle α of the magnetic field direction according to the law $\Delta B = \Delta B_\parallel / cos\alpha$. This law is preserved up to angles of about 60 degrees. Dependence of frequencies of AB oscillations for a 100 nm $Bi_{0.83}Sb_{0.17}$ nanowire at T=1.5 K on the angle α between the direction of applied magnetic field and the wire axis is shown in Fig. 1. The nonmonotonic changes of magnetoresistance, which are equidistant in a direct magnetic field, were observed in transverse magnetic fields under conditions where the magnetic flux through the cylinder Φ=0. Possible reasons for this behavior by analogy with thin bismuth nanowires are discussed.
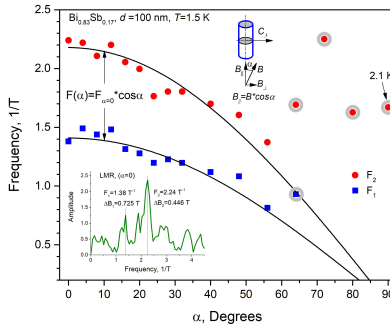

FIG. 1. *Dependence of frequencies of AB oscillations for a 100 nm $Bi_{0.83}Sb_{0.17}$ nanowire at T=1.5 K on the angle α between the direction of applied magnetic field and the wire axis; $\alpha = 0$ corresponds to the longitudinal MR. Frequencies F_1 and F_2 correspond to the MR oscillation with periods Φ_0 and $\Phi_0/2$, respectively. Insert: FFT spectra of the longitudinal MR oscillations.*

[1] L. Konopko, A. Nikolaeva, T. Huber and J.-P. Ansermet, J. Low Temp. Phys., **185**, 673 (2016)

[2] M. Tian *et al.* Sci. Rep. **3**, 1212 (2013)

Poster-Tu11

High quality electrostatically defined hall bars in monolayer graphene

R. Ribeiro-Palau*,[1,2] S. Chen*,[1,3] Y. Zeng,[1] K. Watanabe,[4] T. Taniguchi,[4] J. Hone,[2] and C. R. Dean[1]

[1] Department of Physics, Columbia University, New York, NY, USA

[2] Department of Mechanical Engineering, Columbia University, New York, NY, USA

[3] Department of Applied Physics and Applied Mathematics, Columbia University, New York, NY, USA

[4] National Institute for Materials Science, 1-1 Namiki, Tsukuba, Japan

Realizing graphene's promise as an atomically thin and tunable platform for fundamental studies and future applications in quantum transport requires the ability to electrostatically define the geometry of the structure and control the carrier concentration, without compromising the quality of the system. Here, we demonstrate the working principle of a new generation of high quality gate defined graphene samples, where the challenge of doing so in a gapless semiconductor is overcome by using the $\nu = 0$ insulating state, which emerges at modest applied magnetic fields [1,2]. In order to verify that the quality of our devices is not compromised by the presence of multiple gates we compare the electronic transport response of different sample geometries, paying close attention to fragile quantum states, such as the fractional quantum Hall (FQH) states, that are highly susceptible to disorder, see Fig. 1. Measurements of the energy gaps of the fractional quantum Hall states in different device geometries show a clear decrease of quality when metal gates are used and a dramatic improvement by the use of graphite gates. In addition, these devices permit the first experimental observation of reentrant quantum Hall effect in graphene, revealing the existence of electron solid states in higher Landau levels. This is the first time this electron solid state is observed in other than ultra high quality GaAs/AlGaAs heterostructures. The ability to electrostatically define conducting channels in graphene combined with the high quality of these new structures will enable the study of complex quantum transport phenomena, such as of fractional statistics, in a highly tunable material.
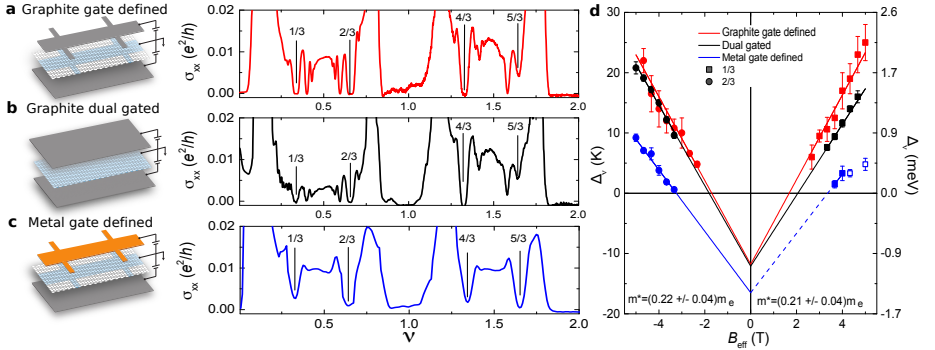

FIG. 1. **FQH states for different device geometries**. Longitudinal conductivity, σ_{xx}, as a function of filling factor at $B = 15$ T and $T = 0.3$ K for: **a**, graphite gate defined, **b**, graphite dual gated devices and **c**, metal gate defined. **d**, Energy gaps for 1/3 and 2/3 fractional quantum Hall states for a graphite gate defined (red), graphite dual gated - second device - (black) and metal gate defined (blue) as a function of the effective field of CF, $B_{eff} = m(B - B_{m/2})$. Solid lines represent linear fit. Dashed blue line represents linear fit of the two lower points of the 1/3 state for the metal gate defined, the other two measurements (empty symbols) seem to be compromised by the proximity of the $\nu = 0$ insulating state. The effective mass was calculated from the cyclotron gap of CF approximation.

[1] A. F. Young *et. al.*, Nat Phys **8**, 550 (2012).

[2] A. F. Young *et. al.*, Nature **505**, 528 (2014).

Poster-Tu12

Field induced phase transitions in the underdoped PrBCO compound in high magnetic fields

Mahieddine Lahoubi,[1] Shengli Pu,[2] and Yongliang Zhao[2]

[1]*Departement de Physique, Laboratoire de Physique du Solide, L.P.S., Université Badji-Mokhtar Annaba, Algerie*

[2]*College of Science, University of Shanghai for Science and Technology, China*

Recently, a detailed magnetic study of the low temperature anomalies in an insulator/semiconductor $PrBa_2Cu_3O_{6+x}$ sample with $x = 0.44$ (henceforth referred to $PrBCO_{6.44}$ for simplicity) was reported by one of us [1]. A significant decrease of the Néel temperature $T_N = 9$ K of the Pr antiferromagnetic (AFM) ordering was revealed with the increase of the magnetic field H. T_N reaches 6-7 K, the temperature region where the T_2-anomaly due to the spin reorientation phase transition is suppressed above 6 T, whereas the transition at the low-critical point $T_{cr} = 4$-5 K associated with the magnetic reordering of the Pr subsystem is still visible when the strength of H is increased up to 10 T. Hence, current attempts to understand the anomalous properties of this underdoped (UN) compound tend to focus on the high magnetic field effects on the transition temperatures T_N, T_2, and T_{cr}.

Therefore, several investigations on the magnetic properties have been made in high magnetic fields using magnetometers based on superconducting coils producing a DC magnetic field H up to 16 T and at several temperatures. The experiments were carried out on the same $PrBCO_{6.44}$ ceramic sample which has been used previously in the measurements of specific heat, thermal expansion and magnetic susceptibility at a very low DC field H = 10 mT [2-4]. The details of preparation and structural characterizations are also given in [2-4]. The isothermal magnetizations $M_T(H)$ measured at 1.35 and 2 K and their differential susceptibilities $dM_T(H)/dH$ versus H obtained by numerical differentiation reveal a weak ferromagnetic (WFM)-like behavior which appears below a field induced phase transition (FIPT) observed at a critical field $H_{cr1} = 3.3$ T. Above H_{cr1}, the WFM is suppressed and the AFM state is established up to $H_{cr2} = 9.25$ T where the FIPT to the paramagnetic state is identified. In addition, the data indicate the presence of a small hysteresis (~ 0.2 T) where the technical magnetization saturation M_{tms} deduced by extrapolation to H = 0 from the linear part of the 1.5-3 T field-range is estimated at about 288 and 293 emu/mol for increasing and decreasing H, respectively.

The temperature dependences up to T_N and few Kelvin above of both $M_{tms}(T)$ and the differential magnetic susceptibility $\chi_d(T)$ in the WFM phase are analyzed and the magnetic phase diagram in the (H-T) plane is reported below T_N. The results are discussed in the frame of the theory of pseudodipole interactions in these exchange-frustrated AFM PrBCO compounds [5] and compared with previous works.

[1] M. Lahoubi, Physica B, Condens. Matter., in Press, doi.org/10.1016/j.physb.2017.10.042
[2] W. Younsi, M. Lahoubi, and M.-L. Soltani, J. Low Temp. Phys., 166, 218, (2012)
[3] M. Lahoubi, S. L. Pu, and D. L. Su, 2015 IEEE International Conference on Applied Superconductivity and Electromagnetic Devices (ASEMD), Nov. 20-23, Shanghai, China, pp. 476–477, Nov. 2015
[4] M. Lahoubi, S. Pu, and D. Su, IEEE Trans. Appl. Supercond., 26, no. 7, Art. no. 7201705 (2016)
[5] S. V. Maleev, JETP Lett., 67, no. 11, 947, (1998)

Poster-Tu13

Effect of photodoping on interlayer exciton in $MoS_2/MoSe_2$ heterostructure

N. Zhang,[1] A. Surrente,[1] M. Baranowski,[1, 2] D. Dumcenco,[3]
Y.-C. Kung,[3] D. K. Maude,[1] A. Kis,[3] and P. Plochocka[1]

[1]*Laboratoire National des Champs Magnétiques Intenses,*
UPR 3228, CNRS-UGA-UPS-INSA, Grenoble and Toulouse, France

[2]*Department of Experimental Physics, Faculty of Fundamental Problems of Technology,*
Wroclaw University of Science and Technology, Wroclaw, Poland

[3]*Electrical Engineering Institute and Institute of Materials Science and Engineering,*
École Polytechnique Fédérale de Lausanne, CH-1015 Lausanne, Switzerland

The direct band gap of monolayer transition metal dichalcogenides (TMDs) as well as their peculiar selection rules, which couple the direct optical transitions in a specific valley with circularly polarized light, make this class of materials interesting for applications in advanced optoelectronic and valleytronic devices. Van der Waals heterostructures can be formed by stacking vertically layered TMDs. Theoretical calculations demonstrate that heterostructures formed of TMDs exhibit a type II band alignment [1]. In these structures, electron-hole pairs formed upon photoexcitation are readily separated in the two layers composing the heterostructure, thereby forming a quasiparticle referred to as interlayer exciton.

In this work, a $MoS_2/MoSe_2/MoS_2$ trilayer heterostructure is prepared by a series of stacking steps of monolayer TMDs grown by chemical vapor deposition (CVD). It has been demonstrated that in TMDs exposure to laser light can change the carrier density. [2] This has been attributed to the interaction between monolayers and the substrate, which generally has a surface rich in charges and dangling bonds. These usually act as donors, which can be optically ionized upon illumination with the laser, leading to a photo-doping effect, which modifies the intensity and energy position of the neutral and charged exciton (trion). We extend the investigation of photo-doping performed on monolayers [2] by examining the effect of laser illumination on the spectrum of $MoSe_2$ intralayer exciton and trion of $MoSe_2$ and on the interlayer exciton. We observed a variation of the exciton to trion PL intensities as well as an increase of the trion dissociation energy over the laser exposure time (see Fig 1(a-c)), which points to a photo-induced doping. Importantly, the variation of carrier density impacts also the emission of the interlayer exciton, as demonstrated by the Fig 1(e), where we show the decrease of the PL intensity of interlayer exciton upon the laser exposure.
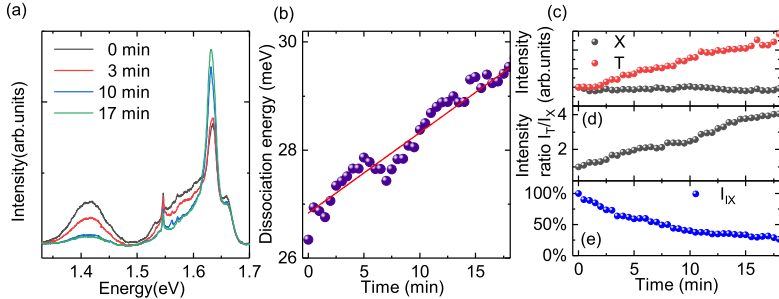

FIG. 1. (a) PL spectra at different exposure time at 4K. (b) Dissociation energy (E_X-E_T) between neutral and charged excitons. (c) Integrated photoluminescence intensity of charged exciton (T, red points) and neutral exciton (X, black points). (d) Ratio between the integrated photoluminescence intensity of T and X as a function of laser exposure time. (e) Integrated photoluminescence intensity of interlayer exciton (IX).

[1] Kang, J. *et al.* Appl. Phys. Lett., **102**, 012111, (2013)

[2] A. A. Mitioglu *et al.* Phys. Rev. B, **88**, 245403, (2013)

Magnetotunneling Characteristics of Imbalanced Double Quantum Wells
in the QHE Regime

G. Schneider[1*], W. Dietsche[2], R. J. Haug[1]

[1]*Institut für Festkörperphysik, Leibniz Universität Hannover, Appelstr. 2, 30167 Hannover, Germany*

[2] *Max Planck Institute for Solid State Research, Heisenbergstr. 1, 70569 Stuttgart, Germany*

Since several years bilayer phenomena such as 2D-2D Tunneling [1], Coulomb drag [2] and excitonic Bose-Einstein condensates (BEC) [3] are observable within double quantum wells in the quantum Hall regime. The BEC was found to arise at balanced layer densities with the filling factor combination of 1/2 and 1/2. In our work we are focusing on imbalanced layers, allowing not only the investigation of the filling factor combination 1/3 and 2/3 but also the system's behavior at various combinations of greater filling factors.

All measurements were performed on a MBE grown GaAs double quantum well separated by a 10 nm AlAs/GaAs barrier. Each layer is individually contacted using field gates for a local depletion [4]. Additional gates allow tuning the charge carrier densities between 1E10 and 4E10 per square centimeter. The interlayer tunneling for imbalanced charge carrier densities is measured and compared to balanced conditions existing inevitable in the samples leads. Measurements were performed at magnetic fields up to three Tesla (reaching below a combined filling factor of one) and for varying density ratios between 33% and 66%. We were able to map the emergence of the excitonic condensate in the filling factor space. Furthermore regions of conductance and insulation were found at combination of higher filling factors which are referable to each layer's individual spin split Quanten Hall state.

[1] N. Turner et al.: Tunneling between parallel two-dimensional electron gases, in: Phys. Rev. B 54(15), (1996).

[2] C. Jörger et al.: Drag effect between 2D electron gases: composite fermion and screening effects, in: Physica E 6 (200)

[3] J.P. Eisenstein and A.H. MacDonald: Bose-Einstein condensation of excitons in bilayer electron systems, in Nature 432, 691-694 (2004)

[4] J.P. Eisenstein et al.: Independently contacted two-dimensional electron systems in double quantum wells, in: Appl. Phys. Lett. 57, 2324 (1990).

* Gunnar Schneider: email: gschneider@nano.uni-hannover.de

Theory of Metal-Insulator Transitions in Graphite Under High Magnetic Field

Zhiming Pan [1], Xiao-Tian Zhang [1] and <u>Ryuichi Shindou</u>[1]

[1]International Center for Quantum Materials, School of Physics, Peking University, Beijing 100871, China (rshindou@pku.edu.cn)

Keywords: spin-nematic excitonic insulators, re-entrant insulator-metal transition,

ABSTRACT

Graphite under high magnetic field exhibits consecutive metal-insulator (MI) transitions as well as re-entrant insulator-metal (IM) transitions in the quasi-quantum limit at low temperature. We introduce models with electron pockets and hole pockets, to construct a bosonized Hamiltonian that comprises of displacement field along the field direction and its conjugate field [1,2]. Using a renormalization group (RG) argument, we show that there exists a critical interaction strength above which a umklapp term becomes relevant and the system enters excitonic insulator phases with long-range ordering of (pseudo)spin superfluid phase field (`spin-nematic excitonic insulator'). We argue that, when a pair of electron and hole pocket become smaller in size in the momentum space, a quantum fluctuation of the spin superfluid phase field becomes larger and eventually destabilizes the excitonic insulator phases, resulting in the re-entrant IM transition [1].
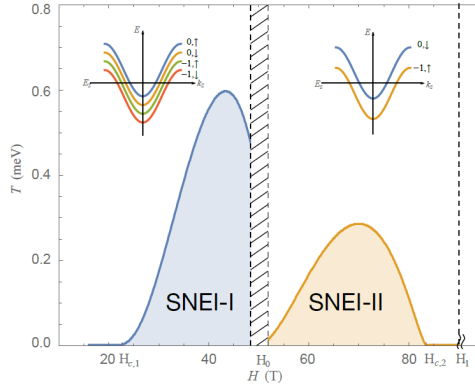
Figure 1: Theoretical Phase Diagram for graphite under high magnetic field. The phase diagram is obtained from the RG analyses. "SNEI-I" and "SNEI-II" stand for two distinct spin nematic excitonic insulator phases.

References

[1] Z. Pan, X.T. Zhang and R. Shindou, "Theory of Metal-Insulator Transitions in Graphite under High Magnetic Field", arXiv:1802.10253

[2] X.T. Zhang and R. Shindou, "Transport properties of density wave phases in three-dimensional metals and semimetals under high magnetic field" Phys. Rev. B 95, 205108 (2017).

Poster-Tu16

Vacuum Bloch-Siegert Shift in Landau Polaritons with Ultrahigh Cooperativity

Xinwei Li,[1] Motoaki Bamba,[2] Qi Zhang,[3] Saeed Fallahi,[4] Geoff C. Gardner,[4] Weilu Gao,[1] Minhan Lou,[1] Katsumasa Yoshioka,[5] Michael J. Manfra,[4] and Junichiro Kono[1]

[1] *Department of Electrical and Computer Engineering, Rice University, USA*

[2] *Department of Materials Engineering Science, Osaka University, Japan*

[3] *Argonne National Laboratories, Lemont, USA*

[4] *Department of Physics and Astronomy, Purdue University, USA*

[5] *Department of Physics, Yokohama National University, Japan*

A Bloch-Siegert shift is a resonance frequency shift that occurs in a pseudospin system when a circularly polarized strong field drives the spin in a counter-rotating manner, i.e., the field and spin interact while rotating in opposite directions [1]. It is typically a minuscule effect and difficult to analyze. Here, we report a vacuum Bloch-Siegert (VBS) shift, which is induced by the ultrastrong coupling of matter with the counter-rotating component of the vacuum fluctuation field in a cavity. Specifically, the cyclotron resonance (CR) of an ultrahigh-mobility two-dimensional electron gas (2DEG) couples ultrastrongly with photons in a high-Q terahertz (THz) cavity in a quantizing magnetic field. Unlike the classical BS shift, we observed an unambiguously large vacuum BS shift up to 40 GHz. From our theory derived from the first principles, we were able to quantitatively analyze the VBS shift and distinguished it from the other unique feature of the ultrastrong coupling regime, i.e., the photon field self-interaction effect due to the A^2 terms. Our observation represents a unique manifestation of a strong-field phenomenon without a strong field.

We performed polarization-resolved transmission time-domain THz magneto-spectroscopy measurements on a hybrid 2DEG-cavity sample at low temperatures. We adopted a photonic crystal cavity structure which was formed by stacking multiple intrinsic silicon wafers with equal spacings. We placed a substrate-removed modulation-doped GaAs quantum well on the central silicon layer, coinciding with the maximum cavity electric field position. We applied an achromatic THz quarter wave plate after the nonlinear THz generation; the THz probe was right-hand circularly polarized (RCP).

Figure 1 shows the Landau polariton dispersion; both experimental transmission peak positions and simulation results are plotted. CR, due to its circular electron motion, has polarization selection rules. RCP THz radiation shows CR absorption in free space at $B > 0$ and is thus CR-active. This resonant coupling led to the well-studied vacuum Rabi splitting (VRS) for $B > 0$ (blue arrows in Fig. 1). However, surprisingly, in the $B < 0$ region, where RCP THz radiation becomes CR-inactive in free space, we still observed a clear shift (red arrows in Fig. 1). Such a frequency shift is not possible unless one considers the coupling of CR with the counter-rotating component of cavity photons. Intuitively, this corresponds to the unusual situation where a THz electric field rotating in the opposite direction to the electron cyclotron motion still strongly couples with the electrons. We identify the frequency shift in the $B < 0$ region as the VBS shift. This is the first clear-cut observation of counter-rotating light-matter coupling in the absence of an intense driving ac field.
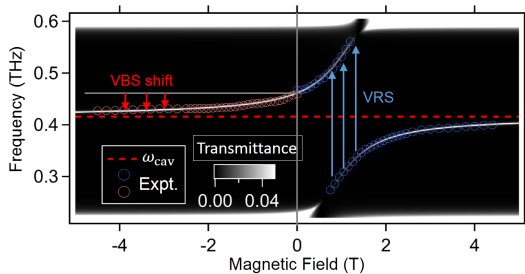

FIG. 1. *Landau polariton dispersion measured with an RCP THz probe. Experimental transmission peak positions (colored circles) are plotted together with simulated transmittance spectra.*

[1] F. Bloch and A. Siegert, Phys. Rev. **57**, 522 (1940).

Poster-Tu17

Spin Mobility in a 2DEG with Persistent Spin Helices

M. Luengo-Kovac,[1] F. C. D. Moraes,[2] G. J. Ferreira,[3] A. S. L. Ribeiro,[2]
G. M. Gusev,[2] A. K. Bakarov,[4] V. Sih,[1] and F. G. G. Hernandez[2]

[1] *Department of Physics, University of Michigan, Ann Arbor, Michigan 48109, United States*

[2] *Instituto de Física, Universidade de São Paulo, São Paulo, SP 05508-090, Brazil*

[3] *Instituto de Física, Universidade Federal de Uberlândia, Uberlândia, MG 38400-902, Brazil*

[4] *Institute of Semiconductor Physics and Novosibirsk State University, Novosibirsk 630090, Russia*

The pursuit for a new active semiconductor component based on flow of spin, rather than that of charge, strongly motivates research in the spintronics field. Since the Datta-Das proposal for a ballistic spin transistor, a full electrical control of the spin state was suggested using the gate-tunable Rashba spin-orbit interaction (SOI). Further studies were developed to make the spin transistor also robust against spin-independent scattering by including the Dresselhaus SOI. For example, it has been demonstrated that SU(2) spin rotation symmetry, preserving the spin polarization, can be obtained when the strengths of the Rashba and Dresselhaus SOI are equal. Drift in those helical systems was recently demonstrated showing also remarkable properties [1].

Nevertheless, spin transport suffers from additional frictional forces, as the spin Coulomb drag, which reduces the possible velocity for a spin package in a given in-plane electric field. This effect appears as a lower mobility for spins than for charge in the same sample. Studies in new systems are thus still necessary to remove this important disadvantage for future devices.

A two-dimensional electron gas (2DEG) hosted in a semiconductor quantum well (QW) with two-subbands occupied introduces new characteristics to the PSH dynamics and offers unexplored opportunities, for example, to create a set of crossed persistent spin helices [2]. Theoretically, two possible scenarios have been found regarding the intersubband scattering (ISS) rate [3].

Here [4], we experimentally studied spin drag in a system with strong ISS where the dynamics is set by the averaged spin-orbit couplings (SOCs) of both subbands. The sample consists of a symmetrically doped wide QW grown in the [001] direction. A device was fabricated in a crossed configuration with two channels along the [1$\bar{1}$0] and [110] crystallographic orientations. The SOCs were tailored in order to attain ortogonal PSHs simultaneously, the first subband in the PSH+ and the second subband in the PSH- (or iPSH). We measured the spin polarization using time-resolved Kerr rotation as function of the space and time separation of pump and probe beams. The application of a drifting in-plane electric field allowed us to determine the spin mobility and the spin-orbit field. As expected in the PSH regime, we observed highly anisotropic spin-orbit fields in the range of several mT and spin mobilities of approximately of $2x10^5 cm^2/Vs$. We were able to control the SOCs in both subbands and to show a linear dependence for the sum of the Rashba constants with the gate voltage. Finally, we determined an inverse relation for the spin mobility dependence on the SOCs. Thus, we directly revealed the additional resistance experienced in the transport of a spin package in a system with uniaxial spin-orbit fields. We modeled our results using a random walk approach and obtained an excellent agreement.

[1] P. Altmann, F.G.G. Hernandez, G.J. Ferreira, M. Kohda, C. Reichl, W. Wegscheider, and G. Salis, Phys. Rev. Lett. **116**, 196802 (2016).

[2] J. Fu, P. H. Penteado, M. O. Hachiya, D. Loss, and J. C. Egues, Phys. Rev. Lett. **117**, 226401 (2016).

[3] G. J. Ferreira, F. G. G. Hernandez, P. Altmann, G. Salis, Phys. Rev. B **95**, 125119 (2017).

[4] M. Luengo-Kovac, F. C. D. Moraes, G. J. Ferreira, A. S. L. Ribeiro, G. M. Gusev, A. K. Bakarov, V. Sih, and F. G. G. Hernandez, Phys Rev. B **95**, 245315 (2017).

Withdrawn-Tu18

Observation of a Wigner crystal and its melting in two-dimensions

Talbot Knighton,[1] Alessandro Serafin,[2] Zhe Wu,[1] J.S. Xia,[2] Loren Pfeiffer,[3] K. W. West,[3] and Jian Huang[1]

[1]*Department of Physics and Astronomy, Wayne State University, Detroit, Michigan, United States of America*

[2]*Department of Physics, University of Florida, Gainesville, Florida, United States of America*

[3]*Department of Electrical Engineering, Princeton University, New Jersey, United States of America*

A Wigner Crystal (WC) [1] in two dimensions (2D) is a long-sought-after solid phase of electrons driven by dominating electron-electron interaction. The melting of a WC provides a unique opportunity of understanding the fundamental quantum solid-liquid phase transition. According to the Mermin-Wagner theory, the long-range order of a 2D classical solid does not survive thermal fluctuations. On the other hand, 2D melting model via unbinding of topological defects (of vortices), known as the Kosterlitz-Thouless (KT) transition, is found and proven in classical systems. A quantum version of the solid phase of electrons is more exotic than the classical version due extra degrees of freedom (i.e. frequency). There has been a long history of attempts making experimental observations of a WC in high-quality 2D semiconductor systems, though there still lacks persuasive evidence due to some outstanding challenges. According to quantum Monte Carlo simulations, a WC emerges only when the inter-particle Coulomb energy (E_c) far exceeds the Fermi energy (E_F), i.e. the ratio $r_s = E_c/E_F$ is beyond 37. Therefore, it requires systems with extremely dilute carrier concentrations, e.g. $\leq 1 \times 10^9$ cm^{-2} for electrons or $\leq 4 \times 10^9$ cm^{-2} for holes in typical GaAs systems. Experiments in such tiny E_c and E_F limits are notoriously difficult because, even apart from quantum fluctuations, the disorder effects, unless effectively suppressed, easily overwhelm the long-range order. Natural consequences are Anderson localization, glasses, and mixed phases none of which possesses true long-range correlation. Most experiments have confirmed these through observing softly pinned modes undergoing a second-order like thermal melting. These modes are characterized by small correlation length and, as broadly suspected, are the result of intermediate or mixed phases. Clear evidence of a WC requires not only large correlation scales, but, moreover, a melting transition marked by a singularity distinguishing the solid and liquid phases [2]. This work presents a first evidence of pinned collective modes, at $r_s > 40$, characterized by a macroscopic correlation length. Moreover, a two-stage melting, analogous to the Kosterilitz-Thouless (KT) model [3], is observed, with a sharp discontinuity across a critical point which suggests a first order nature.

We utilize ultra-high purity p-GaAs 2D systems in which the carrier density can be continuously tuned from 5×10^{10} cm^{-2} down to 7×10^8 cm^{-2}. Effective sample cooling down to 10 mK is achieved via a homemade helium-3 immersion cell. A transport measurement of differential resistance (r_d) is performed for both ultra-dilute systems in a zero-magnetic field (B) and the re-entrant insulating phases in a large B- field. For $T < T_c \approx 30$ mK, collective modes under enormous pinning, characterized by $r_d > 1$ GΩ, are observed, with estimated correlation length up to ~100 micrometers. A remarkably sharp threshold IV is observed at a critical voltage bias, analogous to pinned charge density waves. Thermal melting probed at close to zero bias reveals a piecewise behaviour separated by T_c: a moderate T dependence is displayed from 10 mK up to T_c where a sharp discontinuous drop in r_d takes place. The IV relationship above T_c becomes rounded, in an agreement with previous results. Linear IV is smoothly recovered above $T_l \approx 150$ mK where pinning diminishes and a liquid phase emerges. Melting driven by temperature and electric field will be discussed.
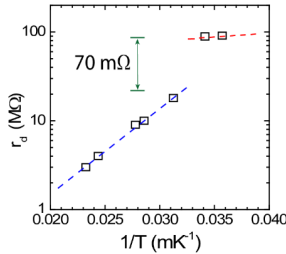

FIG. 1. Discontinuity in the pinning strength, measured via the differential resistance, occurs around $T_c \sim 30$ mK.

[1] E. Wigner, Phys. Rev. 46, 1002 (1934).

[2] P. W. Anderson, Basic Notions of Condensed Matter Physics, Benjamin/Cummings, CA (1984)

[3] J.M. Kosterlitz, J. M., and D. J. Thouless, Journal of Physics C: Solid State Physics 5(11), L124(1972);
    David R. Nelson and B. I. Halperin, Physical Review B 19, 2457 (1979)

Poster-Tu19

Measuring the transmission probability of counterflowing edge channels in InAs quantum Hall systems

Takafumi Akiho, Hiroshi Irie, Koji Onomitsu, and Koji Muraki

NTT Basic Research Laboratories, NTT Corporation, Atsugi, Japan

Understanding and controlling the electronic states near the edge of a two-dimensional system is becoming an increasingly important issue for exploring exotic quasiparticles anticipated to emerge at the edges. Semiconductor heterostructures comprising InAs, which allows for the formation of transparent superconducting junctions, are deemed promising for such purposes [1]. However, the surface potential of InAs can lead to local electron density near the mesa edge higher than the bulk value, which gives rise to counterflowing edge channels in the quantum Hall regime [2] and trivial edge channels in the InAs/(In)GaSb quantum spin Hall insulators [3], thereby compromising the expected transport properties. In this study, we determine the transmission probability of counterflowing edge channels in InAs quantum wells using samples with different edge lengths (l_{edge}) and show that it varies with the edge length, filling factor, and magnetic field in a non-trivial manner.

The sample studied is a 20-nm-thick InAs quantum well sandwiched between AlGaSb barrier layers, processed into front-gated Hall bars having ten Ohmic electrodes and an Al_2O_3 gate insulator. We measured the two-terminal conductance G_F and G_C in the forward and counterflow configurations in the quantum Hall regime, by detecting the currents I_F and I_C using the terminals located downstream and upstream, respectively, of the electrode to which the current (I_{in}) was injected [inset of Fig. 1(a)]. As shown in Fig. 1(a), G_F measured for l_{edge} = 110 μm at 6 T shows a stepwise change as a function of front gate voltage V_{FG}, reflecting the filling factor. G_F shows plateaus around gate voltages close to, but slightly lower than, the values where the bulk filling factor is expected to become integer from Hall resistance measured at 1 T (vertical dashed lines). The most striking observation is that G_C, which should be vanishing in the quantum Hall effect regime, is finite and oscillates with V_{FG}, with maxima reaching values as large as e^2/h. Furthermore, the positions of the minima in G_C are clearly shifted from the integer bulk filling, indicating that the electron density near the mesa edge is higher than in the bulk [4]. Using the Landauer-Büttiker model with counterflowing edge channels, G_C is given in units of e^2/h as the product of the number of counterflowing edge channels (N_C) and the transmission probability (T_C). We performed systematic measurements on different configurations and clarified the l_{edge} dependence of $N_C T_C$ [Fig. 1(b)]. $N_C T_C$ decays exponentially as a function of l_{edge}, with the decay length of about 70 μm at ν = 4 and 6 T. The decay length becomes even longer with increasing magnetic field. In the presentation, we report that the counterflowing edge channel can be suppressed by forming the quantum Hall edge channel by gate voltage rather than mesa edge.
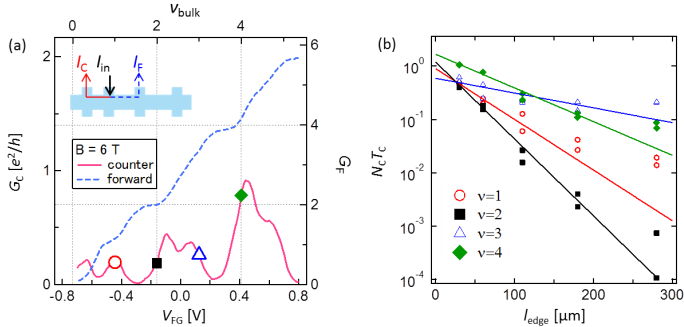
Fig. 1 (a) Front-gate voltage dependence of the conductance measured for l_{edge} = 110 μm in the forward and l_{edge} = 60 μm in the counterflow configurations at B = 6 T and T = 1.5 K. (Inset) measurement configuration. Unused contacts were connected to the ground. (b) Transmission probability of counterflowing edge channels with different edge length. Solid lines are results of fitting.

[1] R. S. K. Mong *et al.*, Phys. Rev. X **4**, 011036 (2014). [2] B. J. van Wees *et al.*, Phys. Rev. B **51**, 7973 (1995).
[3] F. Nichele *et al.*, New J. Phys. **18** 083005 (2016). [4] Y-T. Cui *et al.*, Phys. Rev. Lett. **117**, 186601 (2016).

Poster-Tu20

Carbon nanotubes as excitonic insulators

D. Varsano,[1] S. Sorella,[2] D. Sangalli,[3] M. Barborini,[1] S. Corni,[1] E. Molinari,[1,4] and M. Rontani[1]

[1]*CNR-NANO, Modena, Italy*
[2]*SISSA & CNR-IOM, Trieste, Italy*
[3]*CNR-ISM, Roma, Italy*
[4]*University of Modena and Reggio Emilia, Modena, Italy*

Fifty years ago Walter Kohn speculated [1] that a zero-gap semiconductor might be unstable against the spontaneous generation of excitons—electron-hole pairs bound together by Coulomb attraction (Fig. 1). The reconstructed ground state would then open a gap breaking the symmetry of the underlying lattice, a genuine consequence of electronic correlations. Here we show [2] that this 'excitonic insulator' is realized in zero-gap armchair carbon nanotubes by performing first-principles calculations through many-body perturbation theory as well as quantum Monte Carlo.

We find that the excitonic order modulates the charge between the two carbon sublattices, opening an experimentally observable gap that scales as the inverse of the tube radius. The axial magnetic field provides an experimental handle to switch between excitonic and normal phases, the gap exhibiting a peculiar weak dependence on small fields. Our findings call into question the Luttinger liquid paradigm for nanotubes and provide tests to experimentally discriminate between excitonic and Mott insulator.
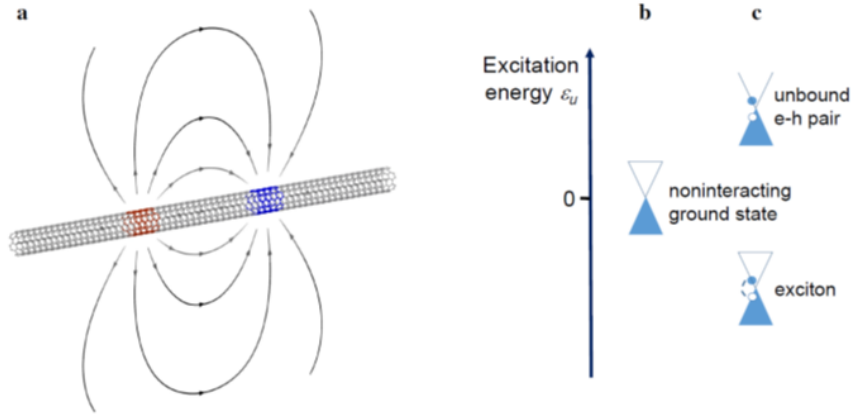

FIG. 1. **Excitonic instability in carbon nanotubes.** (**a**) Sketch of a suspended armchair carbon nanotube. The field lines of the Coulomb force between electron and hole lie mainly in the vacuum, hence screening is heavily suppressed. (**b-c**) Excitonic instability in the armchair carbon nanotube. The scheme represents the excitation energy ε_u of an electron-hole (e-h) pair relative to the noninteracting ground state (b), a zero-gap semiconductor. In the absence of interaction, the excitation energy ε_u of an e-h pair is positive (c). The long-range interaction may bind e-h pairs close to the Dirac point in momentum space. If an exciton forms, then its excitation energy ε_u is negative. This instability leads to the reconstruction of the ground state into an excitonic insulator.

[1] D. Sherrington and W. Kohn, Review of Modern Physics **40,** 767 (1968).
[2] D. Varsano, S. Sorella, D. Sangalli, M. Barborini, S. Corni, E. Molinari, and M. Rontani, Nature Communications **8,** 1461 (2017).

Poster-Tu21

High-field magnetoransport in Eu-doped Bi_2Se_3 thin films with flat defects

B.A. Aronzon[1,2], L.N. Oveshnikov[1,2], Yu.G. Selivanov[2], E.G. Chizhevskii[2]

[1]*National Research Center "Kurchatov institute", 123182 Moscow, Russia*

[2]*P.N. Lebedev Physical Institute RAS, 119991 Moscow, Russia*

We've studied magnetotransport properties of 3D topological insulator (TI) Bi_2Se_3 thin films doped by Eu (0-21at.% calculated for Bi sites) in the wide range of magnetic fields, including high-field region. Magnetically doped TI is much less studied than pure TI materials and in most cases the distribution of magnetic atoms was assumed to be homogenous. In our work we've study systems with highly inhomogeneous distribution of magnetic impurities. Introducing Eu atoms into the film have led to the formation of flat defects, having presumably a pancake-like shape, with thickness about 1 nm. The presence of these defects was observed by means of the transmission electron microscopy [1]. With rise of Eu content, x, the concentration and sizes of defects increases. The electron energy loss spectroscopy results suggest that almost all Eu atoms are localized within these pancake-like defects. At higher x we've also observed the tendency of defects to form stacks of pancakes, in which defects are separated by one or several quint-layers of Bi_2Se_3 matrix.

Magnetotransport properties of Eu-doped films in weak magnetic fields are pretty much similar to those of pure films [2]. We've observed weak antilocalization (WAL) effect without consecutive weak localization for all studied films. But in doped films the dephasing length saturates below 2 K [3], and it's value seems to correlate with the defect concentration. Thus, we assume that the main low-field transport features of TI in our case are conserved due to the locality of magnetic defect interaction with Dirac electrons on the interfaces of the films.

In pure films as we increase magnetic field WAL-related magnetoresistance (MR) turns into a quadratic one already in low-field region. But for Eu-doped films a distinct region of linear MR appears. The width of this region increases with Eu content and for $x = 13\%$ linear MR is observed up to 14 T at $T = 1.4$ K. For $x = 21\%$ the region of linear MR is again equal 15 T at $T = 1.4$ K, it then the region stopped to grow and the presence of linear MR region is questionable. At $x = 21\%$ the range stopped further expansion and if for smaller x at higher magnetic field the dR/dB declines to the up but for $x = 21\%$ to the down. The temperature dependence of linear MR slope has the same form for all samples. Earlier it was suggested that linear MR in Bi_2Se_3 films can be attributed to the superposition of quadratic MR and WAL effect described by complete Hikami-Larkin-Nagaoka formula. But this superposition haven't allowed us to make a good fit of our data. Thus, linear MR in our films can be attributed to a distinct mechanism. But simple estimations showed that common theories of linear MR (such as Abrikosov theory or classical Parish-Littlewood and Stroud-Balagurov models) are not applicable in our case. This is true for the field orientation in direction B_x and B_y but for B_z it is not so (Z is the orientation normal to the film). For B_z the quadratic fit is better description of the experimental date.Thus, the explanation of observed linear MR requires additional theoretical study, especially, if the MR anisotropy of our films is taken onto account.

References
[1] B.A. Aronzon et al., JMMM (2017). https://doi.org/10.1016/j.jmmm.2017.09.058
[2] L.N. Oveshnikov et al., JETP Lett. 104(9), 629-634 (2016).
[3] L.N. Oveshnikov et al., JETP Lett. 106(8), 526-533 (2017).

Hall effect sign reversal within voids in semiconductors

R. G. Mani,[1] A. Kriisa,[1] C. Reichl,[2] W. Wegscheider,[2]

[1]*Dept. of Physics & Astronomy, Georgia State University, Atlanta, GA 30303*

[2]*Laboratorium für Festkörperphysik, ETH-Zürich, 8093 Zürich, Switzerland*

Recent experimental work has examined the possibility of realizing sign reversal of the Hall coefficient in metamaterials.[1,2] The idea here is to coax an n-type material to exhibit a p-type Hall effect. The results have captured the popular imagination given the long history, fundamental importance in research and applications, and simplicity of the Hall effect.[3,4] The possibility of Hall effect inversion was theoretically refined by Brian and Milton,[5] through the examination of the effective conductivity of a composite material. They apparently proved that it was possible for certain properties such as the Hall effect to change sign in a composite. Since the report of this finding, there has been great interest in the realization of sign reversal in the Hall effect/Hall coefficient.[1-9]

Following upon this interest, we re-examine the possibility of Hall effect/Hall coefficient sign reversal in traditional, non-composite semiconducting- and metallic- 2D and 3D systems.[6-8] Based on measurements in the GaAs/AlGaAs 2D electronic system and bulk GaAs, we show that it is possible to realize Hall effect sign reversal in canonical semiconducting systems, as in metamaterials. That is, it is possible for an n-type material to show a p-type Hall effect. To realize this sign reversal, we place a material void in a semiconducting plate and insert contacts on the interior of the void, as in the metamaterial system.[1] When a current is injected through the interior of the void, a sign reversed classical Hall effect/coefficient can be realized on the interior boundary Hall effect contacts.[6-8]

Hall devices can be rendered ineffective for sensing by offset voltages, which are caused by contact misalignment that appear across the Hall contacts even in the absence of a magnetic field. Generating sign reversed Hall effects within voids can be useful for engineering the distribution of current so as to reduce such offset voltages, increasing magnetic-field sensitivity.[6-8]
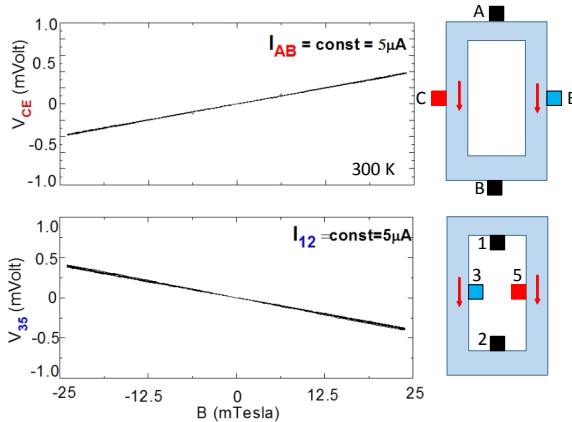

Fig. 1. Hall effect in a specimen with a void. Top – Current is injected via contacts {A,B} and the Hall effect is measured via contacts {C,E}. Bottom - Current is injected via contacts {1,2} and Hall effect is measured via contacts {3,5}. Note the Hall-sign reversal between the effects measured on the interior- and the exterior- of the void.

[1] C. Kern et al., Phy. Rev. Lett. **118**, 016601 (2017).
[2] M. Kadic et al., Phys. Rev. X **5**, 021030 (2015).
[3] J. L. Miller, Phys. Today **70** (2), 21 (2017).
[4] M. Notomi, Nature **544**, 44 (2017).
[5] M. Briane and G. W. Milton, Arch. Rational. Mech. Anal. **193,** 715 (2009).
[6] R. G. Mani, Phys. Today **70** (7) 13, (2017).
[7] R. G. Mani and A. Kriisa, Nature **548**, 31 (2017).
[8] A. Kriisa et al., IEEE Trans. Nanotech. **10**, 179 (2011); AIP Conf. Proc. **1566**, 195 (2013).
[9] M. Wegener et al., Phys. Today **70** (10), 14 (2017).

Poster-Tu23

Possible Topological Phases in an Organic Dirac Fermion System

Toshihito Osada, Ayaka Mori, Kenta Yoshimura, and Mitsuyuki Sato

Institute for Solid State Physics, University of Tokyo, Kashiwa, Japan

A layered organic conductor, α-(BEDT-TTF)$_2$I$_3$, is known as a two-dimensional Dirac fermion system, which shows a topological quantum Hall ferromagnetic state at high magnetic fields [1]. We propose the emergence of other topological states, the Chern insulator phase and the topological insulator phase, in this system. These are organic analogues of the Haldane model [2] and the Kane-Mele model [3] in graphene.

First, we discuss the possible Chern insulator phase in the weak charge order (CO) state in the vicinity of CO transition [4]. We assume a pattern of site potential and staggered magnetic flux on the α-(BEDT-TTF)$_2$I$_3$ lattice to reproduce the observed potential and magnetic modulations [5] (Fig. 1(b)). We shows that under large enough magnetic modulation, the system becomes a Chern insulator, where gaps open at two Dirac points (Fig. 1(c)), and one chiral edge state appears along each crystal edge (Fig. 1(e)). The conduction through these edge states successfully explains the anomalous metallic behavior of resistance observed in the weak CO state around the critical pressure (Fig. 1(a)).

Next, we show that the Z$_2$ topological insulator state emerges at low temperatures with the spin-orbit interaction. Valenti *et al.* discussed that the finite spin-orbit interaction opens gaps at Dirac points causing the insulating behavior observed at low temperatures [6] (Fig. 1(a)). We assume inter-molecular hopping including the spin-orbit interaction on the α-(BEDT-TTF)$_2$I$_3$ lattice reflecting the observed charge disproportionation. We demonstrate that gaps open at Dirac points and one helical edge state appears along each crystal edge. Moreover, we generally discuss the appearance of the topological insulator based on the Fu-Kane parity product theory [7].
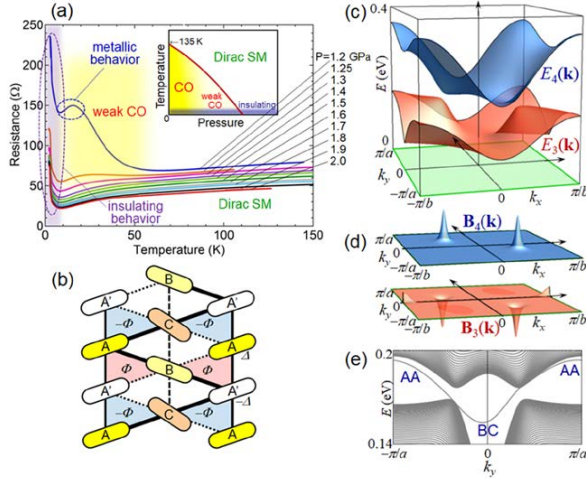

FIG. 1. (a) Temperature dependence of interlayer resistance in α-(BEDT-TTF)$_2$I$_3$ under several pressures. The resistance shows the metallic behavior in weak charge order (CO) insulating state. The inset shows a schematic phase diagram. (b) Schematic crystal lattice of the conduction layer in α-(BEDT-TTF)$_2$I$_3$. The additional site potential (Δ, $-\Delta$) and magnetic flux (Φ, $-\Phi$) due to charge ordering are indicated. (c) Energy dispersion of the valence band $E_3(\mathbf{k})$ and conduction band $E_4(\mathbf{k})$ when $\Delta=0$ and $\Phi=0.025h/e$. Gaps open at two valleys. (d) Berry curvature of the valence and conduction bands. The Berry curvature peaks at two valleys have the same sign, resulting in the quantum anomalous Hall effect. (e) Energy spectrum of the nanoribbon with AA' and BC edges. One chiral edge state appears along each edge.

[1] T. Osada, J. Phys. Soc. Jpn. **84**, 053704 (2015).
[2] F. D. M. Haldane, Phys. Rev. Lett. **61**, 2015 (1988).
[3] C. L. Kane and E. J. Mele, Phys. Rev. Lett. **95**, 226801 (2005).
[4] T. Osada, J. Phys. Soc. Jpn. **86**, 123702 (2017).
[5] K. Ishikawa et al., Phys. Rev. B **94**, 085154 (2016).
[6] S. M. Winter, *et al.*, Phys. Rev. B **95**, 060404 (2017).
[7] L. Fu and C. L. Kane, Phys. Rev. B **76**, 045302 (2007).

Novel two-component fractional quantum Hall effect in double-layer graphene

J.I.A Li[1], T. Taniguchi[2], K. Watanabe[2], J. Hone[3] and C.R. Dean[1]

[1] Physics Department, Columbia University, New York, NY, USA

[2] National Institute for Materials Science, 1-1 Namiki, Tsukuba, Japan

[3] Department of Mechanical Engineering, Columbia University, New York, NY, USA

A graphene double layer structure is achieved by bringing two monolayer graphene in close vicinity, separated by a tunneling barrier that is ~2nm thick. The strong interlayer Coulomb interaction provides an ideal platform to explore ground state with exotic order, including, but not limited to, exciton condensate [1]. In this talk, I will present recent transport measurements in double-layer graphene structure, where the close vicinity between two monolayer graphene induces strong interlayer Coulomb interaction and stabilizes exotic 2-component fractional quantum Hall effect [2]. The ground state in graphene double layer is tunable with magnetic field, interlayer separation, filling fractions and density imbalance, providing us with a multi-dimensional phase space to characterize and study these novel states of matters. Most notably, parallel flow and counterflow measurements offers key insights of the interlayer pairing mechanism that gives rise to the interlayer phase coherence. Additionally, we observe a phase transition between 2-component ground states to a composite fermion sequence of FQHE with decreasing interlayer Coulomb coupling. Our results establish the first experimental study of the tunability and ground state order of two-component fractional quantum Hall effect in graphene double-layer, and demonstrated the complex landscape of phase transitions between these novel states of matter.
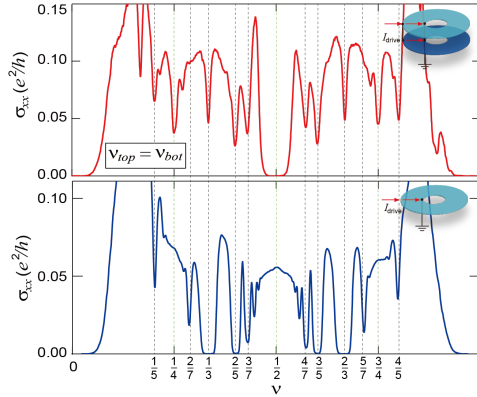

Figure 1, longitudinal conductance measured in corbino geometry for double-layer graphene (upper panel) compared to monolayer graphene (lower panel). As a result of strong interlayer Coulomb coupling, the sequence of two-component FQHE is distinctively different from the composite fermion sequence in monolayer graphene.

[1] J. I. A. Li, T. Taniguchi, K. Watanabe, J. Hone, and C. R. Dean, Nat. Phys. 13, 751 (2017).

[2] J. I. A. Li, T. Taniguchi, K. Watanabe, J. Hone, and C. R. Dean, in preparation (2018).

Poster-Tu25

Correlated quantum dot in external magnetic field: an effective non-stationary spin filter

V.N. Mantsevich,[1] N.S. Maslova,[1] P.I. Arseysv[2]

[1]*Lomonosov Moscow State University, Moscow Russia*

[2]*P.N. Lebedev Physical Institute of RAS, Moscow, Russia*

One of the key issues of spintronics is the control and generation of spin-polarized currents. Nowadays generation and detection of spin-polarized currents in semiconductor nanostructures has attracted great attention since this is the key problem in developing semiconductor spintronic devices [1,2]. Such systems integration in a little quantum circuits requires careful analysis of non-stationary effects, transient processes and time evolution peculiarities of initially prepared charge and spin states. Non-stationary electron transport in nano-scale systems is strongly governed by localized electrons Coulomb interaction, which also influence the characteristics of stationary state. Moreover, the presence of external fields can strongly modify charge, spin and local magnetic moment kinetics in the single and coupled QDs. To analyze the local magnetic moment, each spin electron occupation numbers and total charge in the correlated single-level quantum dot (QD) coupled to reservoir in the presence of external magnetic field we applied the non-stationary kinetic equations for localized electron occupation numbers and their correlation functions, taking into account all high-order correlation functions for the localized electrons. The simplest way to obtain the system of kinetic equations is the Heisenberg approach.

We have shown that time evolution of local magnetic moment, each spin electron occupation numbers and total charge in the correlated single-level quantum dot (QD) coupled to reservoir is quite different for shallow and deep energy level in the presence of magnetic field. Relaxation regimes for magnetic field switching "on" strongly differ from ones when magnetic field is switched "off". It was demonstrated that depending on the energy level position and the strength of magnetic field different relaxation regimes are present in the system. For the QD with deep energy level and weak magnetic field long living local magnetic moment and each spin electron occupation numbers are present both for switching "on" and "off" of magnetic field. For deep energy level and strong magnetic field relaxation rates of local magnetic moment and each spin electron occupation numbers for magnetic field switching "on" strongly differ from the situation when magnetic field is switched "off". Such an asymmetry was not found for QD with shallow energy level. Moreover, long living magnetic moment can't exist in the system with shallow levels. Obtained results provide possibility for dynamic memory devices stabilization in the presence of magnetic field and, consequently, improving the reliability of data storing [3].

We have also analyzed the behavior of spin-polarized non-stationary currents in the system of single-level quantum dot situated between two non-magnetic electronic reservoirs with Coulomb correlations of localized electrons in the presence of external magnetic field switched "on" or "off" at particular time moment. It was demonstrated that single-level correlated quantum dot can be considered as an effective spin filter depending on the ration between the values of magnetic field induced energy level splitting and applied bias voltage [4].

[1] G.A. Prinz, Science 82, 1660, (1998).
[2] P. Chuang et.al., Nat. Nanotechnol. 10, 35, (2015).
[3] V.N. Mantsevich et.al., Journal of Magnetism and Magnetic Materials, accepted for publication (2018).
[4] V.N. Mantsevich et.al., Physica E, 93, 224, (2017).

Poster-Tu26

Existence of Aharonov-Bohm interferometry at a single p-n junction in quantum Hall graphene

Nojoon Myoung[1] and Hee Chul Park[2]

[1]*Department of Physic Education, Chosun University, Gwanju 61452, Republic of Korea*

[2]*Center for Theoretical Physics of Complex Systems,
Institute for Basic Science, Daejeon 34126, Republic of Korea*

Graphene is a promising material for studying quantum Hall effects with gate-tunable filling factors on account of its capability for controlling charge density via field effects[1]. It has been well known that the topological invariant (or so-called Chern number) of a quantum Hall insulator is given by the filling factor in the integer quantum Hall effect [2]. The observation of noninteger conductance plateaus in bipolar graphene quantum Hall systems has been interpreted by the equilibration of interface states at the pn junction, with theoretical efforts supporting experimental findings by considering edge and interface disorders [3]. Mesoscopic conductance fluctuation should therefore be expected to appear in the coherent regime, e.g., a valley-isospin dependence of the quantum Hall effects in graphene p-n junctions [4].

In this study, the transport properties of Chern insulator junctions generated by bipolar junctions in quantum Hall graphene are theoretically studied in the coherent regime. Coherent transport across the junction exhibits two mesoscopic features: valley-isospin dependence of the quantum Hall conductance, and the Aharonov-Bohm (AB) effects with the interface channels. We demonstrate that the valley-isospin dependence can be measured in a graphene sample with perfect edge terminations, resulting in conductance oscillation for the smallest Chern number case. On the other hand, while conductance plateaus are found to be unclear for larger Chern numbers, the conductance exhibits an oscillatory behavior of which period is relatively longer than the valley-isospin dependent oscillation, as shown in Fig. 1(a). This conductance oscillation is ascribed to the AB effect, which is implicitly created by the split metallic channels near the junction interface. (see Fig. 1(b-d)) We point out that a possible origin of the unclear plateaus previously speculated to be incompleteness in realistic devices is the low-visibility conductance oscillation due to unequal beam splitting.
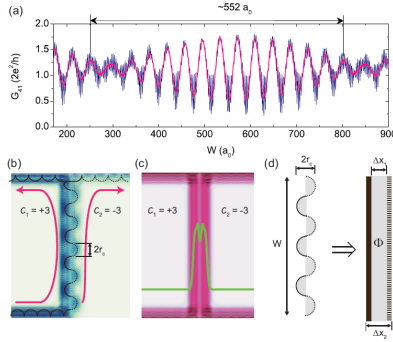

FIG. 1.   *(a) Beat of the conductance across the junction for given potential as a function of interface length W. (b) Probability density map at $E_F = 0$ for an incoming mode from the left of the bottom edge, with illustrations of the pathway of the metallic channels and the corresponding semiclassical skipping motions. (c) Local density of states map corresponding to (b). (d) Schematics of the implicit Aharonov-Bohm interferometry.*

[1] A. K. Novoselov *et al.* Nature (London), **438**, 197, (2005)

[2] D. J. Thouless *et al.* Phys. Rev. Lett. **49**, 405, (1982)

[3] J. Li and S.-Q. Shen *et al.* Phys. Rev. B **78**, 205308 (2008)

[4] J. Tworzydlo *et al.* Phys. Rev. B **76**, 035411 (2007)

Poster-Tu27

Non-linear Zeeman effect for infrared intracenter transitions in ^{11}B doped diamond

Sergey Tarelkin,[1,2] Vitaly Bormashov,[1,3] Sergey G. Pavlov,[4] Dmytro L. Kamenskyi,[5] Dmitry Prikhodko,[1,6] Mikhail Kuznetsov,[1] Sergey Terentiev,[1] Martin Wienold,[4,7] Heinz-Wilhelm Hübers,[4,7] and Vladimir Blank[1,2,6]

[1] *Technological Institute for Superhard and Novel Carbon Materials, Troitsk, Moscow, Russia*
[2] *National University of Science and Technology MISiS, Moscow, Russia*
[3] *The All-Russian Research Institute for Optical and Physical Measurements, Moscow, Russia*
[4] *Institute of Optical Sensor Systems, German Aerospace Center (DLR), Berlin, Germany*
[5] *High Field Magnet Laboratory (HFML - EMFL), Radboud University, Nijmegen, The Netherlands*
[6] *Moscow Institute of Physics and Technology, Dolgoprudny, Moscow Region, Russia*
[7] *Humboldt-Universität zu Berlin, Institut für Physik, Berlin, Germany*

Zeeman effect is one of the powerful experimental techniques providing key information on the symmetry of electronic states of impurity centers in semiconductors. While the structure of most conventional impurities in elemental semiconductors has been studied for a long time and is accurately known, boron as a hydrogen-like acceptor in diamond, is less explored and the electronic structure of its excited levels is not yet precisely known. Zeeman effect of the electronic Raman transition between spin-orbit split even-parity states of boron acceptors ground state (GS) in a natural type IIb-type diamond has been studied for the magnetic field (up to 7T) parallel to different cubic axes of a crystal [1]. Recently, we studied influence of magnetic field on infrared (IR) intracenter transitions (3-4 µm range) in synthetic HPHT (high-pressure high-temperature growth technique) diamond [2]. Due to limited spectral resolution, concentration and isotopic broadenings (presence of ^{10}B and ^{11}B centers) of impurity transitions only linear evolution with a field of the boron ground states was observed.

Here we present the low temperature magneto-optical spectroscopy study of a IIb-type synthetic diamond doped by isotopically enriched ^{11}B. The measurements were done on a HPHT IIb-type single crystal diamond (001) wedged plate. The ^{11}B boron concentration was about 2×10^{17}cm^{-3} that notably reduces the number of acceptor transitions. Measurements were done with a temperature control in the 2-10 K range in the 30 T water-cooled Bitter magnet at the HFML, Nijmegen, The Netherlands. Mid-IR radiation from a Fourier spectrometer (Bruker IFS-113v, a globar source, Ge-KBr beam splitter) was guided to the sample by an evacuated beam-line and detected by a Si bolometer built-in in a cryogenic optical dipstick. The light propagates parallel to the magnetic field and perpendicular to the sample surface (the Faraday geometry). Transmission spectra were collected with 1 cm^{-1} spectral resolution up to 30 T with a 2 T step.

The main boron-related optical transitions revealed clear Zeeman splitting into several components. Some of the excited states exhibit non-linear field dependence, clearly observed at B > 10 T. The temperature evolution of the spectra allowed us to distinguish the transitions originated from a 2 meV spin-orbit split Γ_7 ground state due to its thermal population.

The experimental results will be processed using the known evolution of the boron ground state and its thermal population estimated at different temperatures. On the basis of the Zeeman evolution, the symmetry of several excited states will be clarified.

[1] Kim H. *et al.* Phys. Rev. B., **62**, 12 (2000)
[2] Tarelkin S.A. *et al* Diam. Relat. Mater., **75**, 52, (2017)

Poster-Tu28

Anomaly in the quantum Hall effect in the HgTe/CdHgTe double quantum well

M.V. Yakunin,[1] S.S. Krishtopenko,[2] S.M. Podgornykh,[1] M.R. Popov,[1] V.N. Neverov,[1] F. Teppe,[3] B. Jouault,[3] W. Desrat,[3] N.N. Mikhailov,[4] and S.A. Dvoretsky[4]

[1]*Institute of Metal Physics, Ekaterinburg, Russia*

[2]*Institute for Physics of Microstructures, Nizhny Novgorod, Russia*

[3]*Laboratoire Charles Coulomb (L2C), UMR CNRS 5221, Universite Montpellier, 34095 Montpellier, France*

[4]*Institute of Semiconductor Physics, Novosibirsk, Russia*

The uniqueness of the energy spectrum of the HgTe quantum well and its strong dependence on the well width allows us to construct various versions of the nontrivial energy structure in the HgTe/CdHgTe double quantum well (DQW). This may be useful for a variety of applications, as well as for researching fundamental effects under new conditions. For example, in a DQW with relatively wide HgTe layers (20 nm), it is possible to create an enhanced overlap of the conductivity and valence subbands, which may be controlled by the gate voltage V_g [1]. As a result, the critical field of opening the gap shifts to higher fields where it falls into the well-pronounced regime of the quantum Hall effect (QHE). Under these conditions, specific features like a multiple inversion of QHE and a stable transition into a zero filling factor state were revealed, which may be explained in terms of the mixed electron and hole nature of magnetic levels.

Particularly bright anomalies in the structure of QHE were found in the DQW with HgTe layers of critical thickness (6.5 nm) [2]. In this case, the DQW energy spectrum resembles that of a bilayer graphene, but with its own additional features and a possibility to modify it. A peculiar structure of QHE was revealed here manifesting a combination of two different regimes in a single magnetoresistance (MR) plot (Fig. 1): one for fully free holes (at high fields where the 2–1 plateau–plateau transition shifts with V_g) and the other for a case of partial localization of holes into the lateral maxima (LM) of the valence subband (in relatively weak fields where the structures are almost insensitive to V_g). A transition between the two ranges of fields manifests a reentrant behavior of QHE as MR returns to the same plateau with a change in magnetic field. We show, on the basis of detailed calculations of the energy spectra and the patterns of magnetic levels, that the observed anomaly in QHE is caused by a combination of two factors: the proximity of the Fermi level to LM and the imposition of an electron level on a set of the light holes levels. Insensitivity of QHE to V_g at low fields is due to a high density of states in the vicinity of LM while at higher fields the Fermi level rises in energy to the higher lying hole magnetic levels thus leaving the high density area. Evolution of the observed anomalous structure with V_g was investigated in detail. It was found that the DQW profile is initially asymmetric but it is made symmetric at $V_g = +3$ V. The experimental picture of the MR evolution with field and V_g contains characteristic points that correspond to specific points in the calculated magnetic level pattern, thus the realistic DQW profile may be corrected while making these features coincide.
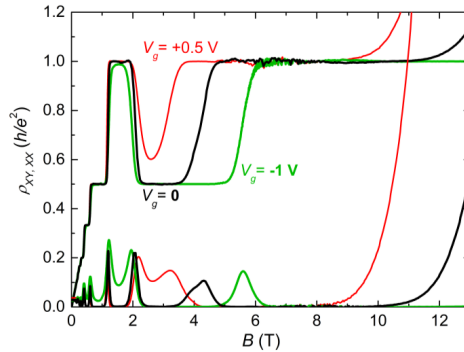

FIG. 1. The picture of the reentrant quantum Hall effect in the HgTe/CdHgTe DQW. Note that only the high-field 2–1 plateau–plateau transition reacts on the gate voltage V_g. Temperature is 0.3 K.

[1] M.V. Yakunin *et al.* Phys. Rev. B, **93**, 085308 (2016).
[2] M.V. Yakunin *et al.* JETP Letters, **104**, 403 (2016).

Poster-Tu29

Temperature dependence of the small and narrow negative magnetoresistance effect about null magnetic field in the quasi-ballistic GaAs/AlGaAs 2DES.

Rasanga. L. Samaraweera[1], Binuka Gunawardana[1], Annika Kriisa[1], Tharanga Nanayakkara[1], Rasadi Munasinghe[1],

Christian Reichl[2], W. Wegscheider[2] & Ramesh G. Mani[1]

[1]Dept. of Physics and Astronomy, Georgia State University, Atlanta, GA 30303
[2]Laboratorium für Festkörperphysik, ETH-Zürich, 8093 Zürich, Switzerland

Both the radiation induced magnetoresistance (MR) effects, and the dark magneto-transport properties of the ultra-high mobility quasi-ballistic GaAs/AlGaAs 2D system, in the low magnetic field limit, have attracted recent experimental attention [1,2]. Here, we examine a small and narrow negative magnetoresistance in the GaAs/AlGaAs 2DES, that appears roughly over the field range of $-0.025 \leq B \leq 0.025$ T, as a function of sample temperature from 1.7 K to 20.0 K. This aim of the work is to study the effect of temperature on the narrow negative-MR effect and determine whether WL type line-shape analysis succeeds in describing the data. Thus, we fit the narrow negative-MR data using the method of Hikami by neglecting the spin orbit scattering term and electron-electron interaction effects [3]. The experimental data are well described by such Hikami lineshape fits and fit extracted inelastic length appears to decrease rapidly with temperature. Observed narrow negative-MR effect are quenched by about T = 20 K The extracted inelastic lengths are compared with the single particle scattering length, which was determined from line-shape fits of the Shubnikov-de Haas oscillations [4], in order to determine whether small angle scattering is responsible for the apparent weak-localization signature in this narrow negative-MR effect.
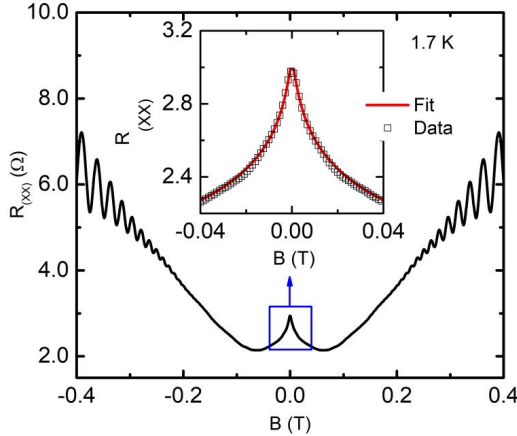

FIG. 1. Narrow negative-magnetoresistance effect about null magnetic field in the high mobility GaAs/AlGaAs 2D system. The inset shows the enlarged view of the data (squares) and the fit (solid line) using 2D WL theory by Hikami.

[1] R. G. Mani et al. Nature. 420, 646-650 (2002)
[2] R. G. Mani, A. Kriisa, and W. Wegscheider, Sci. Rep. 3, 2747 (2013)
[3] S. Hikami, A. I. Larkin, & Y. Nagoaka, Prog. Theor. Phys. 63, 707-710 (1980)
[4] R. G. Mani & J. R. Anderson, Phys. Rev. B. 137 4299-4302 (1988)

Poster-Tu30

Bichromatic microwave induced magnetoresistance oscillations in high mobility GaAs/AlGaAs 2D electron systems

Binuka Gunawardana,[1] C. R. Munasinghe,[1] R. L. Samaraweera,[1] T. R. Nanayakkara,[1] A. Krissa,[1] U.K. Wijewardana,[1] C. Reichl,[2] W. Wegscheider,[2] and R. G. Mani[1]

[1]*Department of Physics and Astronomy, Georgia State University, Atlanta, GA 30303*

[2]*Laboratorium für Festkörperphysik, ETH Zürich, CH-8093 Zürich, Switzerland*

Microwave induced magnetoresistance oscillations in 2D electron systems have been studied intensively to obtain a better understanding of the origin of the associated radiation-induced zero-resistance states.[1,2] A topic of interest in this area has been the study of the physical response under bi- and multi- chromatic excitation. Thus, we have examined the bi-chromatic response as a function of the microwave power at both frequencies using a highly sensitive derivative technique, see Fig. 1(a), that allows the study of the oscillatory response even at extremely low magnetic fields. Half-cycle plots of the oscillatory extrema dRxx/dB with respect to the inverse magnetic field, see Fig. 1(b), clearly establish that the low frequency monochromatic response dominates at low magnetic field regions as the high frequency monochromatic response dominates at high magnetic field regions.
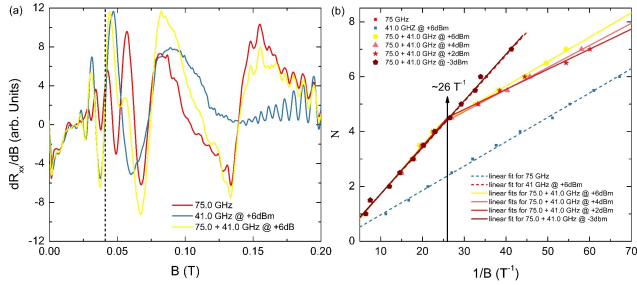

FIG. 1. (a) dR_{xx}/dB is plotted vs. B for monochromatic and bichromatic excitation at 75.0 GHz and 41.0 GHz at the specified power level. (b) This panel shows half-cycle plots, i.e., plots of the extremal index vs. B^{-1}, for the monochromatic cases along with bichromatic excitation with 41.0 GHz as +6, +4, +2 and -3dBm

[1] R. G. Mani et al., Nature, 420, 646 (2002).

[2] B. Gunawardana, H.-C. Liu, R. L. Samaraweera, M. S. Heimbeck, H. O. Everitt, J. Iarrea, C. Reichl, W. Wegscheider and R. G. Mani, Phys. Rev. B. 95, 195304 (2017).

Poster-Tu31

Effect of carrier heating induced by current bias in the regime of Shubnikov de Haas oscillations in the high mobility GaAs/AlGaAs 2D electron systems

C. Rasadi Munasinghe,[1] Binuka Gunawardana,[1] R. L. Samaraweera,[1] T. R. Nanayakkara,[1] A. Kriisa,[1] U.K. Wijewardana,[1] S. Vithanage,[1] C. Reichl,[2] W. Wegscheider,[2] and R. G. Mani[1]

[1]*Department of Physics and Astronomy, Georgia State University, Atlanta, GA 30303*

[2]*Laboratorium für Festkörperphysik, ETH Zürich, CH-8093 Zürich, Switzerland*

The ultra-high mobility GaAs/AlGaAs 2D electron system has served as the host for many new physical phenomena in condensed matter physics. Recent investigations of steady state non-equilibrium phenomena have produced new interest in the magnitude and role of electron heating induced by photo-excitation or current bias. Hence, we trace the joule heating effect through a study the background subtracted diagonal resistance (ΔR_{xx}) in the GaAs/AlGaAs 2D electron system in the regime of Shubnikov-de Haas (SdH) oscillations to determine the influence of a relatively low ac bias on the carrier temperature. The change in the amplitudes of SdH oscillations with the ac bias at different bath temperatures ($0.2\ K \leq T_b \leq 4.2\ K$) was analyzed to extract the elevated electron temperature.[1] GaAs/AlGaAs Hall bar devices including segments with different widths were measured to determine the size dependence of the current bias induced electron heating. Results indicate that a steady state non-equilibrium hot electron situation can be induced by an ac bias current and increased electron temperature is linearly proportional to the ac current, and it is size dependent. These factors can be accounted using a model where the electron-electron scattering is the dominant pathway for energy relaxation, with a secondary role for energy relaxation by electron-phonon coupling.[2]
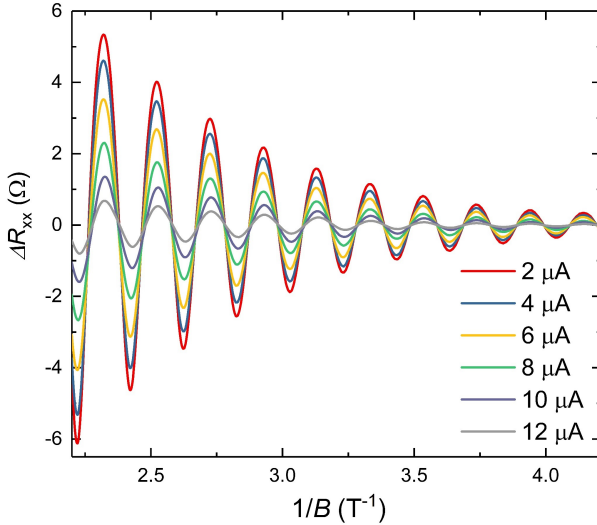
FIG. 1. *The figure shows the background subtracted diagonal resistance versus the inverse magnetic field at different bias currents in a GaAs/AlGaAs 2D device.*

[1] A. N. Ramanayaka, R. G. Mani, and W. Wegscheider, Phys. Rev. B **83** 165303 (2011)

[2] X. L. Lei, and S. Y. Liu, Phys. Rev. B **72** 075345 (2005)

Poster-Tu32

Microwave photo-excitation induced electron heating in the GaAs/AlGaAs 2D electron system

Tharanga Nanayakkara,[1] Rasanga Samaraweera,[1] Binuka Gunawardana,[1] C. Rasadi Munasinghe,[1] Kushan

Wijewardane,[1] Sajith Vithanage,[1] Annika Kriisa,[1] Christian Reichl,[2] Werner Wegscheider,[2] and

Ramesh G. Mani [1]

[1]*Department of Physics and Astronomy, Georgia State University, Atlanta, GA 30303*

[2]*Laboratorium für Festkörperphysik, ETH-Zürich, 8093 Zürich, Switzerland*

We study the enhancement of the zero magnetic field diagonal resistance and the concurrent reduction in the amplitude of Shubnikov-de Haas (SdH) oscillations within the range of $2.3\omega < \omega_c \leq 5.2\omega$, where $\omega_c = eB/m^*$, $\omega = 2\pi f$, B is the magnetic field, m^* is the effective mass, and f is microwave frequency, in the GaAs/AlGaAs 2D electron system (2DES) under microwave irradiation, when energy absorption from the microwaves field serves to heat the carriers in the 2DES, see Figure 1. In this work, we quantitatively analyze the heating effect as a function of the incident microwave intensity. The electron temperature is extracted from the SdH oscillations by fitting the SdH lineshape, as the electron temperature at zero magnetic field were determined by comparing with the resistance variation with the lattice temperature.

The results show that microwave produces a small discernable increase in the electron temperature both at zero magnetic field and at examined SdH range in the GaAs/AlGaAs 2DES. The heating effect at zero magnetic field appears greater in comparison to the heating effect at finite magnetic fields, in the examined SdH field interval, in line with theoretical predictions [1,2], although the increase in the electron temperature in the zero-field limit appears smaller than theoretical predictions. In addition, the results imply a dependence of the heating effect at zero magnetic field on the microwave frequency, with enhanced heating at lower frequencies. Such a frequency dependence is not observed, however, at finite magnetic fields. Such results will be compared with theory [1,2].
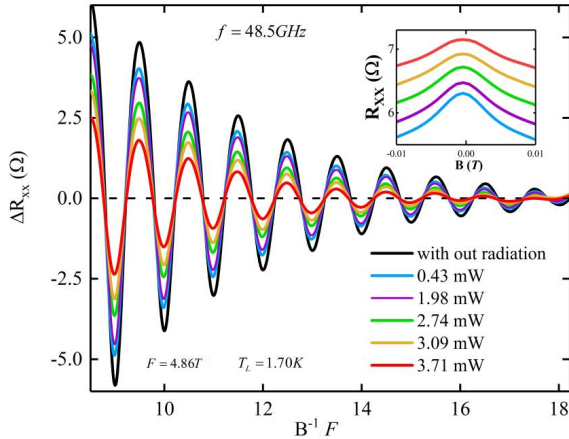

FIG. 1. Decay of the Shubnikov-de Haas oscillation amplitude in the GaAs/AlGaAs high mobility 2DES as a function of the microwave intensity at the lattice temperature T_L=1.7 K. The incident microwave frequency is 48.5 GHz. (Top right) Insert shows the zero-magnetic field longitudinal resistance shifting up with incident microwave power increment.

[1] X. L. Lei and S. Y. Liu, Phys. Rev. B 72, 075345 (2005)

[2] R. G. Mani, Appl. Phys. Lett. 91, 132103 (2007)

[3] X. L. Lei and S. Y. Liu, Appl. Phys. Lett. 94, 232107 (2009)

Poster-Tu33

Magnetotransport of modulation-doped $Al_{0.2}Ga_{0.8}Sb$/GaSb structures

Laura Hanks, Leonid Ponomarenko, Andrew R J Marshall, and Manus Hayne

[1]Department of Physics, Lancaster University, Lancaster LA1 4YB, United Kingdom

GaSb/AlGaSb, the unknown relative of the famous GaAs/AlGaAs system, has been under-researched in the field of electronic devices, despite promising properties of low effective mass and high dielectric constant which would allow the creation of high mobility devices [1]. GaSb investigations have been extensive in the field of optoelectronics, but limited to only basic bulk studies in the field of magnetotransport [2]. More advanced structures, such as two-dimensional electron gases (2DEGs) formed from heterojunction and quantum well structures are being realised in this work, through simulation, growth and measurement, with the objective of studying magnetotransport properties of GaSb/AlGaSb 2DEGs for the first time.

Theoretical band structures and transport results using Nextnano software [3] for GaSb/$Al_{0.2}Ga_{0.8}Sb$ heterostructures will be presented, in which variations of doping concentration, background impurity concentration and spacer thickness were explored. The most promising structures were then grown by molecular beam epitaxy. However, measurements yielded a higher than expected background defect acceptor level and ultimately resulted in p-type devices. A subsequent GaSb growth trial was undertaken to explore the variation of these inherent GaSb defects with growth conditions [4]. The gallium antisite is doubly accepting and in high concentration, and it was found that the reduction of these defects is the key to achieving high-mobility, n-type devices.

With new knowledge of the material properties, revised simulations are being performed with the aim of improving transport properties in a GaSb/$Al_{0.2}Ga_{0.8}Sb$ 2DEGs, results of which will be presented at the conference.
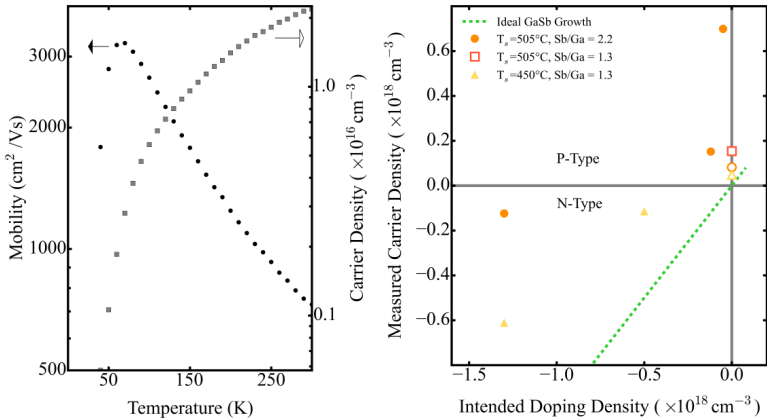
FIG. 1. Left. Mobility as a function of temperature for a GaSb/$Al_{0.2}Ga_{0.8}Sb$ slab doped heterojunction (●) with the associated carrier density (■). Right. Measured carrier density against intended carrier density at room temperature for 3 growth conditions to display the native defects occurring in GaSb, the legend shows the substrate temperature and the V/III ratio for each condition. Undoped samples are shown as open symbols and the ideal GaSb growth, shown as a dashed line, is a 1:1 relationship between intended carrier density and measured carrier density.

[1]Takeda et al. J. Appl. Phys., 24, L455, (1985)
[2]Marshall et al. Infrared Physics & Technology, 70, 168, (2014)
[3]Birner et al. Acta. Phys. Polonica. A, 110, 111, (2006)
[4]Hanks, et al. J. Phys. Conf. Ser., 964, 012006 (2018)

MAGNETORESISTANCE IN HEAVILY DOPED SEMICONDUCTORS

Antonio Ferreira da Silva[1,*], Bo Evert Sernelius[2], Alexandre Levine[3], Eduard Levinson[3] and Henri Boudinov[4]

[1]Instituto de Fisica, Universidade Federal da Bahia, Salvador, BA, Brazil
[2]Department of Physics, Chemistry and Biology,Linköping University,Sweden
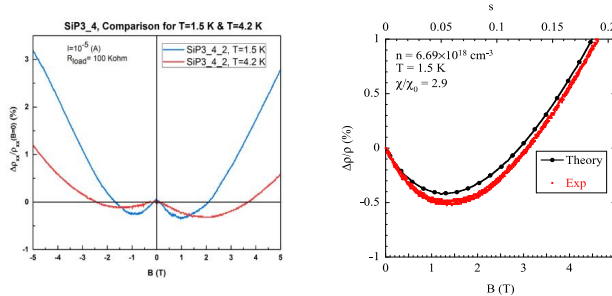[3]Instituto de Física, Universidade de São Paulo, São Paulo, SP, Brazil
[4]Instituto de Fisica, Universidade Federal do Rio Grande do Sul, PA,RS, Brazil
* **Presenting Author, e-mail: ferreira.fis@gmail.com**

More recent discoveries on magnetoresistance as the colossal magnetoresistance (CMR) [1], the extraordinary magnetoresistance (EMR) [2], and the large magnetoresistance (LMR) [3,4]. All these spectacular properties were found in either magnetic systems or in special geometrical structures. In our interpretation of the anomalous behavior point to many-body effects [5]. We have performed magnetoresistance measurements and many-body theoretical calculations assuming n-type doping at the bottom of the many-valley conduction band and above the MNM transition. We have obtained the impurity concentrations by ion implantation process.

For all conducting pure single crystals it is experimentally found that the application of a magnetic induction **B** results in an increase of the resistivity, ρ; the magnetoresistance ratio, or just magnetoresistance, defined as $\Delta\rho/\rho=[\rho(B)-\rho(0)]/\rho(0)$ is positive. This general behavior of the crystalline state is in sharp contrast to the conduction properties of a number of heavily doped semiconductors where one observes a negative magneto-resistance as in this work involving n-type Si and Ge. As example we show in Figures below the heavily doped n-type silicon Magnetoresistance at 1.5 and 2.4 K in the presence of magnetic field.

References

[1] A. P. Ramirez, J. Phys. Condens. Matter **9**, 8171 (1997).
[2] S. A. Solin, T. Thio, D. R. Hines, and J. J. Heremans, Science **289**, 1530 (2000).
[3] M. N. Ali et all., Nature (London) **514**, 205 (2014).
[4] T. Wang et all., AIP Advances 7, 056604 (2017)
[5] A. Ferreira da Silva, A. Levine, Z. Sadre Momtaz, H. Boudinov, and B. E. Sernelius, Phys. Rev. B **91**, 214414 (2015).

Super-long-living spin excitations in a purely electronic two-dimensional spin-unpolarized gas in a strong magnetic field.

Sergey Dickmann

Institute of Solid State Physics RAS, Chernogolovka, Moscow Region, Russia

The lowest-energy excitation in a $\nu = 2$ quantum Hall system is a purely electronic cyclotron spin-flip exciton (CSFE) [1] where electron is promoted from the upper spin sublevel (with 'spin-down') of the zero Landau level to the next Landau level with 'spin-up'. The CSFE energy is well smaller than the cyclotron one: it is separated from upper magnetoplasma mode by a negative Coulomb shift (1mV) and from the ground state by a gap of $\approx 5-7\,\mathrm{mV}$. The q-momentum dispersion of the CSFE energy is rather weak and has a smooth minimum at $q = q_0 \approx 1/l_B$ (l_B is the magnetic length [1]). The considerable Coulomb shift consists of two negative contributions: the first one is the zero-momentum $q = 0$ shift determined only by the second-order Coulomb correction [2]; and the second part is the first-order correction at a finite momentum [1]. Both contributions at $q \approx q_0$ are approximately equal. At low temperature (actually at $T < 0.1\,\mathrm{mK}$) the CSFE can only relax with the emission of hard acoustic phonons [3]. An extremely long life of the state is determined by the following reasons: (i) the studied relaxation is simultaneously the energy and spin relaxation process – the CSFE is a 'dark' exciton, radiative relaxation is suppressed; (ii) the state is energetically far from the ground state, so emitted phonons possessing a very short wavelength are only weakly coupling to the state. A theoretical estimate yields the characteristic CSFE relaxation time expected to reach several milliseconds. At higher temperatures a radiative mechanism of the relaxation is switched on via thermal-activation transition to the upper magnetoplasma state fast-relaxing radiatively. As a result, experimentally even at $T > 0.4\,\mathrm{mK}$ the CSFE relaxation (actually the spin relaxation) can occur with the characteristic time of 100 mcs [4] — still super long for unconfined systems consisting of free conduction-band electrons. In the works [4-5] the CSFE relaxation and kinetics are studied both experimentally and theoretically. The dense CSFE ensemble (with the CSFE number N_x reaching ten percents of the number of magnetic flux quanta N_ϕ) is created by means of the resonant photoexcitation pumping. To monitor the CSFE ensemble state, an additional time-resolved technique of the photoinduced resonant absorption/reflection (PRA/R) is employed. Experimentally, at a given CSFE concentration $n = N_x/N_\phi$ above 5 percents a threshold enhancement of the PIRA/R signal is observed when the temperature is dropping below some value $T_0 = T(n)$ within the $0.4\,\mathrm{K} < T < 1\,\mathrm{K}$ range. This effect can be explained in the framework of a CSFE-ensemble phase transition to a coherent state — bosonic condensate. Theory describes both incoherent and coherent states in terms of the so-called excitonic representation (see Refs. [2,3] and the Supplementary Note 1 in Ref. [5]) and gives a tenfold increase in the PIRA/R signal during the CSFE-ensemble transition to the condensate state (i.e. to a Bose-condensate formed in a purely electronic system). The theory estimation agrees with the experimental data.

[1] C. Kallin and B.I. Halperin, Phys. Rev. B 30, 5655 (1984).
[2] S. Dickmann and I.V. Kukushkin, Phys. Rev. B 71, 241310(R) (2005).
[3] S. Dickmann, Phys. Rev. Lett. 110, 166801 (2013).
[4] L.V. Kulik , A.V. Gorbunov, A.S. Zhuravlev, V.B. Timofeev, S. Dickmann, & I.V. Kukushkin, Nature Sci. Rep. 5, 10354 (2015).
[5] L.V. Kulik, A.S. Zhuravlev, S. Dickmann, A.V. Gorbunov, V.B. Timofeev, I.V. Kukushkin, S. Schmult, Nature Comm. 7, 13499 (2016).

Poster-Tu36

Topological order in quantum phases in anisotropic Kagome magnets

Tohru Kawarabayashi,[1] Kota Ishii,[1] and Yasuhiro Hatsugai[2]

[1] *Department of Physics, Toho University, Funabashi, Japan*

[2] *Division of Physics, University of Tsukuba, Tsukuba, Japan*

A plateau structure of the magnetization curves at 1/3 of the full magnetization is one of the remarkable properties of antiferromagnetic systems on the Kagome lattice. Among quantum states with the average magnetization 1/3 on the Kagome lattice, a tripartite entangled plaquette state has been proposed for a spin-1/2 XXZ model on an anisotropic Kagome lattice [1] . The tripartite entangled plaquette state is expected to be adiabatically connected to a product state of the three-qubit states [2] $|W\rangle = (|\uparrow\downarrow\downarrow\rangle + |\downarrow\uparrow\downarrow\rangle + |\downarrow\downarrow\uparrow\rangle)/\sqrt{3}$ of the three spins on the triangle, where the symmetry of the Hamiltonian is fully preserved.

To distinguish this tripartite plaquette state from other states such as the valence-bond solid state and a ferromagnetic state with the average magnetization 1/3, we examine the fractionally quantized Berry phase [3-5] as a possible topological order parameter to characterize the tripartite entangled plaquette state. We carry out the Lanczos method to obtain the exact ground state of the Hamiltonian of the system with 27 spins and evaluate the Z_3 Berry phase [3] for an up triangle of the Kagome lattice. We then find that the Z_3 Berry phase shows a transition from 0 to $2\pi/3$ when the anisotropy of the antiferromagnetic coupling is increased (Fig.1). The present results are consistent with the existence of the tripartite entangled plaquette state in an anisotropic regime since the Z_3 Berry phase becomes $2\pi/3$ in the product state of the $|W\rangle$ states, which is expected to be the ground state in the strongly anisotropic limit of the present model. While our estimation of the critical value of J_1 turns out to be smaller than that estimated by the large-scale Monte Carlo technique [1] for the transition from the ferromagnetic phase to the tripartite entangled plaquette state, this may be attributed to the smallness of the present system-sizes accessible by the exact diagonalization method.
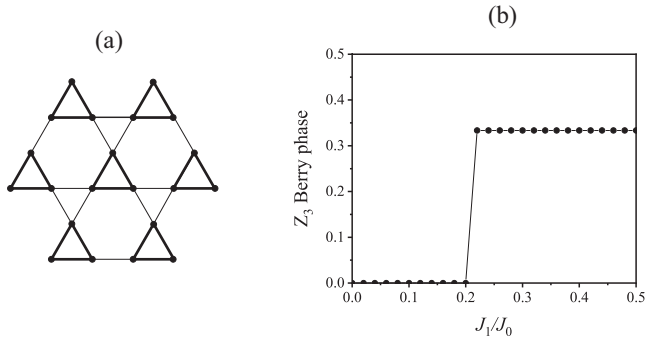

FIG. 1.   (a) The Kagome lattice where the anisotropic spin-1/2 XXZ model is described by the Hamiltonian $H = \sum_{<i,j>\in\triangle} J_1 S_{zi}S_{jz} + \sum_{<i,j>\in\triangledown} J_2 S_{zi}S_{jz} - \sum_{<i,j>}(J_0/2)(S_i^+S_j^- + S_i^-S_j^+)$. Here $S_{ix}(S_{iy}, S_{iz})$ stands for the x(y,z)-component of the spin at the site i and $S_i^{\pm} = S_{ix} \pm iS_{iy}$. The coupling $J_1(J_2)$ describes the antiferromagnetic interaction in the up(down) triangles of the Kagome lattice indicated by the thick(thin) lines. (b) The fractionally quantized berry phase in units of 2π for $J_2/J_0 = 0.1$. The Berry phase shows a transition from 0 to $2\pi/3$ at $J_1/J_0 \sim 0.2$.

[1] J. Carrasquilla, G. Chen, and R. Melko, Phys. Rev. B**96**, 054405 (2017). [2] W. Gür *et al.*, Phys. Rev. A **62**, 062314 (2000). [3] Y. Hatsugai and I. Maruyama, Europhys. Lett. **95**, 20003 (2011). [4] T. Kariyado and Y. Hatsugai, Phys. Rev. B90, 085132 (2014); Phys. Rev. B91, 214410 (2015). [5] T. Kariyado, T. Moritomo, and Y. Hatsugai, arXiv:1709.01546.

	Sunday 22 July	Monday 23 July	Tuesday 24 July	Wednesday 25 July	Thursday 26 July	Friday 27 July
8h50		Opening				
9h00		P. Kim	N. Hussey	M. Yankowitz	T. Heinz	B. Béri
9h30		T. Szkopek	L.E. Golub	C. Dean	A. Arora	Lyand-Geller
9h45		M.V.Durnev	T. Khouri	L.Lzulakowska	J. Holler	F.Appugliese
10h00		J. Lau	D. Smirnov	B.Urbaszek	A. Mitioglu	S. Chen
10h15		E. Henriksen	S.Wiedmann	M.R. Molas	Slobodeniuk	M. Novak
10h30		Coffee break				
11h00		A. Young	A. Coldea	N. Wang	G. Gusev	L. Weiss
11h30		Y. Zhang	P. Sessi	M. Glazov	A. Suslov	O.Makarovsky
1200		Buffet Lunch	Buffet Lunch	Conference Excursion with packed lunch	Buffet Lunch	Closing
14h00		G. Yusa	R.McDonald		A. Surrente	
14h30		B. Fauqué	T. Story		A. Akrap	
15h00		T. Taen	K.S.Denisov		M. Naumann	
15h15		N. Han Tu	F. Telesio		Shahrokhvand	
15h30		X. Liu	K. Rubi		D.K. Efetov	
15h45		S. Crooker	R.Masutomi		F.Parmentier	
16h00		Coffee	Coffee		Coffee	
16h30		Shot gun 1 + Poster Session Mo + Cocktail dinatoire	Shot gun 2 + Poster Session Tu + Cocktail dinatoire		A.Gorbunov	
16h45					J. Oswald	
17h00					V.Gavrilenko	
17h15					M. Zudov	
17h30						
18h00	Welcome reception NOVOTEL					
20h00				Reception/ Banquet		
21h00						